

HFHF

Transport coefficients and evolution of QGP phase at finite baryon density

Olga Soloveva



P. Moreau, L. Oliva, T. Song, I. Grishmanovskii,
V. Voronyuk, V. Kireyeu, E. Bratkovskaya

In collaboration with D. Fuseau, J. Aichelin



14 September 2022
Castiglione della Pescaia
Italy

Properties of QGP: transport coefficients

"Numerical simulations are now essential to make contact between theory and experiment" - J. Kapusta SQM 22

! One has to specify transport and microscopic properties as well as EoS for theoretical simulations of HICs (hydro / transport approaches)



EoS(ϵ, n)
 $\sigma(\sqrt{s}, m_q, m_q, T, \mu_B)$
 $m(T, \mu_B)$

On practice: effective models
for QGP

Transport simulations with QGP phase:

Catania transport – QuasiParticle Model

F. Scardina, S. K. Das, V. Minissale, S. Plumari, and V. Greco,
PRC 96, 044905 (2017).



– Dynamical QPM for partonic phase

W. Cassing, E. Bratkovskaya, PRC 78 (2008) 034919
P. Moreau, O. S, L. Oliva, T. Song, W. Cassing, E. Bratkovskaya,
PRC 100 (2019) , 014911;
O. S, P. Moreau, L. Oliva, V. Voronyuk, V. Kireyeu, T. Song,
E. Bratkovskaya, Particles 3 (2020), 178-192

AMPT – PNJL EoS (Mean field potentials)

K.J. Sun, C. M. Ko, and Z.-W. Lin, PRC 103(2021)

Hybrid simulations with QGP:

vHLLE/MUSIC+UrQMD/SMASH

Iu.A. Karpenko, P. Huovinen, H. Petersen and M. Bleicher
PRC 91 (2015), 064901.

S. Ryu, J.F.Paquet, C. Shen, G.S. Denicol, B. Schenke
PRL 115 (2015), 132301

Properties of QGP: transport coefficients



$EoS(\epsilon, n)$
 $\sigma(\sqrt{s}, m_q, m_q, T, \mu_B)$
 $m(T, \mu_B)$

On practice: effective models
for QGP

Today:

Transport coefficients at finite T and μ_B

- 1.) crossover, CEP and 1st order phase transition ($N_f = 3$ PNJL model)
- 2.) crossover + CEP ($N_f = 3$ DQPM)



— Dynamical QPM for partonic phase

W. Cassing, E. Bratkovskaya, PRC 78 (2008) 034919
P. Moreau, O. S, L. Oliva, T. Song, W. Cassing, E. Bratkovskaya,
PRC 100 (2019) , 014911;
O. S, P. Moreau, L. Oliva, V. Voronyuk, V. Kireyeu, T. Song,
E. Bratkovskaya, Particles 3 (2020), 178-192

Properties of QGP: transport coefficients

Hydrodynamics

$$\begin{cases} \partial_\mu T^{\mu\nu} = 0 & T^{\mu\nu} = -Pg^{\mu\nu} + wu^\mu u^\nu + \Delta T^{\mu\nu} \\ \partial_\mu J_B^\mu = 0 & J_B^\mu = n_B u^\mu + \Delta J_B^\mu \end{cases}$$

$$\eta (D^\mu u^\nu + D^\nu u^\mu + \frac{2}{3} \Delta^{\mu\nu} \partial_\rho u^\rho) - \zeta \Delta^{\mu\nu} \partial_\rho u^\rho$$

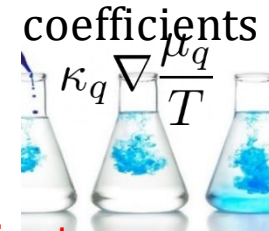
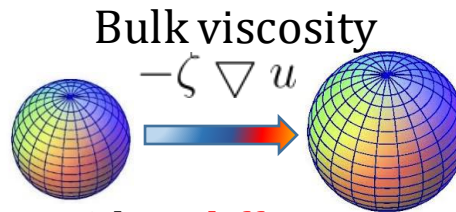
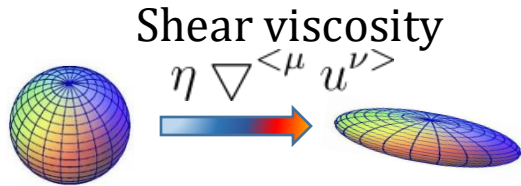
$$\Delta J_B^\mu = \kappa_B D^\mu (\frac{\mu_B}{T})$$

input for hydro

Transport coefficients:

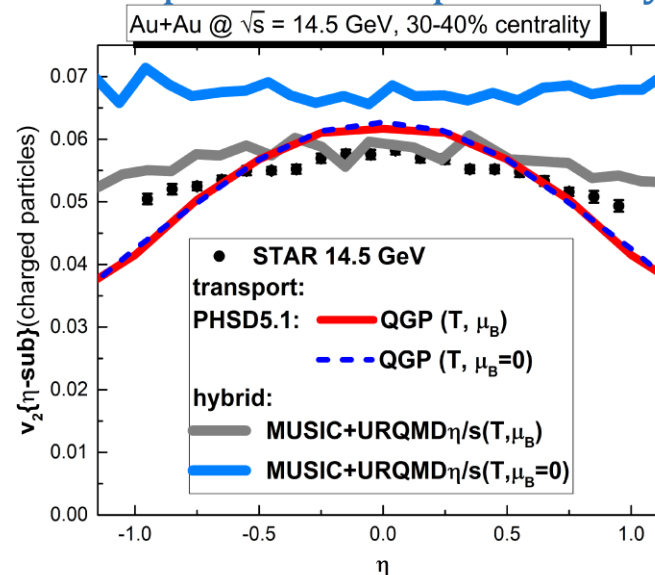
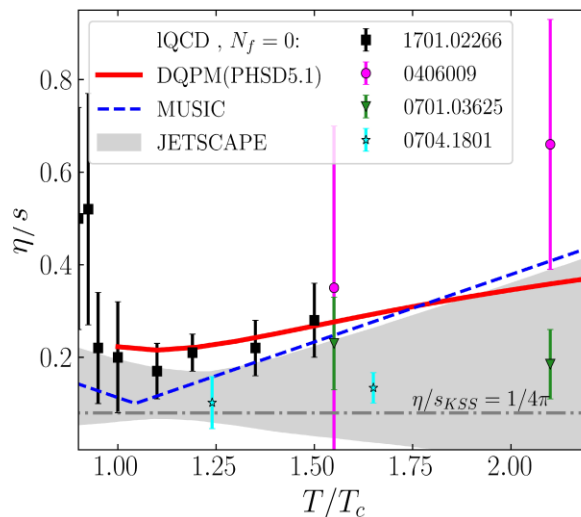
(B, Q, S) diffusion

coefficients
 $\kappa_q \nabla \frac{\mu_q}{T}$

Model predictions for QGP: ! same EoS but different transport coefficients

Transport coefficients can serve a bridge for comparison transport and hydro



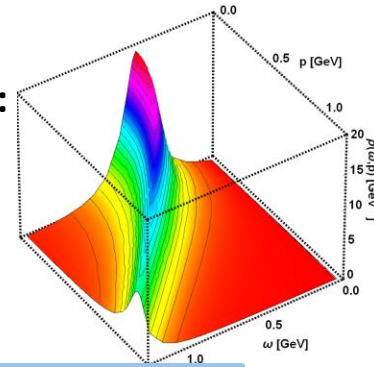
MUSIC:
 C. Shen,
 S. Alzhrani, PRC
 102 (2020) 1,
 014909

Dynamical Quasi-Particle Model

The QGP phase is described in terms of strongly-interacting quasiparticles - quarks and gluons with Lorentzian spectral functions:

$$\rho_j(\omega, \mathbf{p}) = \frac{\gamma_j}{\tilde{E}_j} \left(\frac{1}{(\omega - \tilde{E}_j)^2 + \gamma_j^2} - \frac{1}{(\omega + \tilde{E}_j)^2 + \gamma_j^2} \right)$$

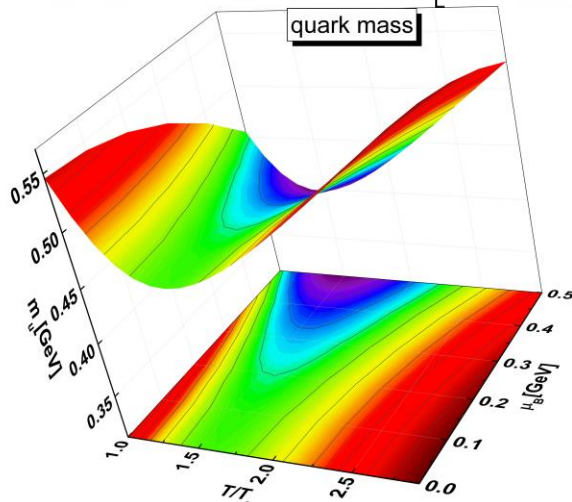
$$\equiv \frac{4\omega\gamma_j}{(\omega^2 - \mathbf{p}^2 - M_j^2)^2 + 4\gamma_j^2\omega^2}$$



resummed propagators: $\Delta_i(\omega, \mathbf{p}) = \frac{1}{\omega^2 - \mathbf{p}^2 - \Pi_i}$ & self-energies: $\Pi_i = m_i^2 - 2i\gamma_i\omega$

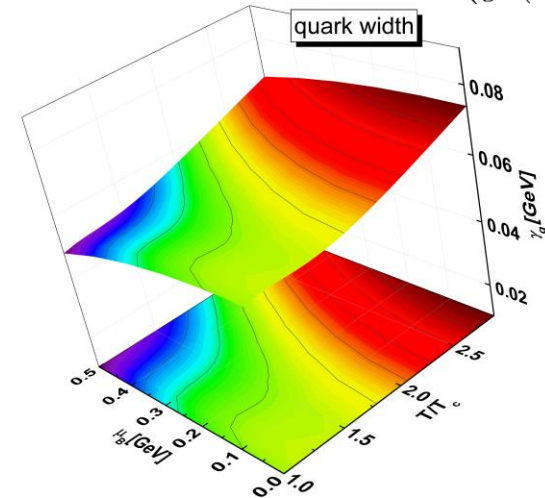
Re Π_i : thermal mass (M_g, M_q)

$$m_{q(\bar{q})}^2(T, \mu_B) = C_q \frac{g^2(T, \mu_B)}{4} T^2 \left[1 + \left(\frac{\mu_B}{3\pi T} \right)^2 \right]$$



Im Π_i : interaction width (γ_g, γ_q)

$$\gamma_j(T, \mu_B) = \frac{1}{3} C_j \frac{g^2(T, \mu_B) T}{8\pi} \ln \left(\frac{2c_m}{g^2(T, \mu_B)} + 1 \right)$$



DQPM: EoS

Entropy and baryon density in the quasiparticle limit
(G. Baym 1998, Blaizot et al. 2001):

$$s^{dqp} = - \int \frac{d\omega}{2\pi} \frac{d^3p}{(2\pi)^3} \left[d_g \frac{\partial n_B}{\partial T} (\text{Im}(\ln -\underline{\Delta}^{-1}) + \text{Im} \underline{\Pi} \text{Re} \underline{\Delta}) \right. \\ \left. + \sum_{q=u,d,s} d_q \frac{\partial n_F(\omega - \mu_q)}{\partial T} (\text{Im}(\ln -\underline{S}_q^{-1}) + \text{Im} \underline{\Sigma}_q \text{Re} \underline{S}_q) \right. \\ \left. + \sum_{\bar{q}=\bar{u},\bar{d},\bar{s}} d_{\bar{q}} \frac{\partial n_F(\omega + \mu_q)}{\partial T} (\text{Im}(\ln -\underline{S}_{\bar{q}}^{-1}) + \text{Im} \underline{\Sigma}_{\bar{q}} \text{Re} \underline{S}_{\bar{q}}) \right]$$

$$n^{dqp} = - \int \frac{d\omega}{2\pi} \frac{d^3p}{(2\pi)^3} \left[\sum_{q=u,d,s} d_q \frac{\partial n_F(\omega - \mu_q)}{\partial \mu_q} (\text{Im}(\ln -\underline{S}_q^{-1}) + \text{Im} \underline{\Sigma}_q \text{Re} \underline{S}_q) \right. \\ \left. + \sum_{\bar{q}=\bar{u},\bar{d},\bar{s}} d_{\bar{q}} \frac{\partial n_F(\omega + \mu_q)}{\partial \mu_q} (\text{Im}(\ln -\underline{S}_{\bar{q}}^{-1}) + \text{Im} \underline{\Sigma}_{\bar{q}} \text{Re} \underline{S}_{\bar{q}}) \right]$$

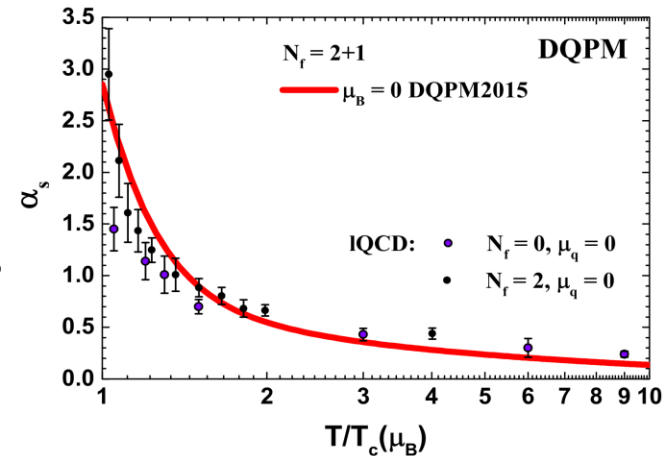
➤ Input: entropy density as a $f(T, \mu_B = 0)$

$$g^2(s/s_{SB}) = d((s/s_{SB})^e - 1)^f \quad \text{fix the parameters}$$

$$s^{DQPM}(\Pi, \Delta, S_q, \Sigma) = s^{lattice}$$

➤ Scaling hypothesis for the **crossover region** at finite μ_B

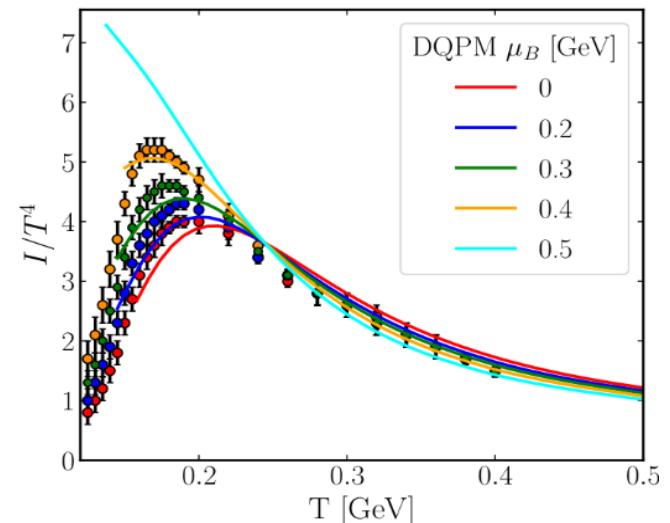
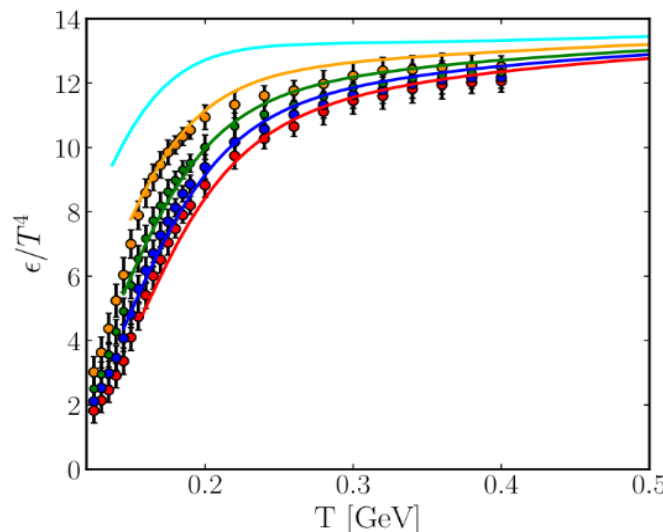
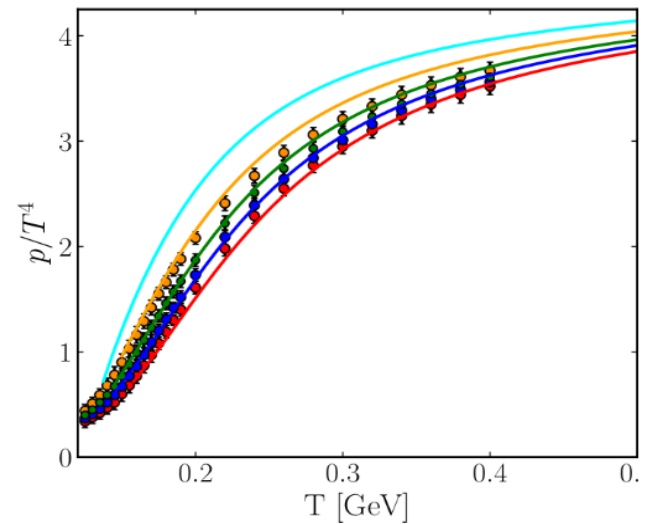
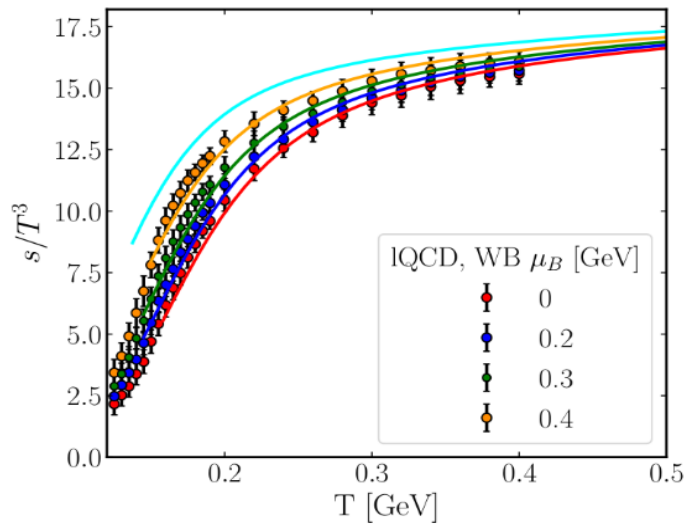
$$g^2(T/T_c, \mu_B) = g^2\left(\frac{T^*}{T_c(\mu_B)}, \mu_B = 0\right) \quad \text{with} \quad T^* = \sqrt{T^2 + \mu_q^2/\pi^2}$$



DQPM: EoS

Input:
lattice EoS
 $\mu_B = 0$
(red dots)

Output:
DQPM EoS
 $\mu_B \geq 0$
(lines)

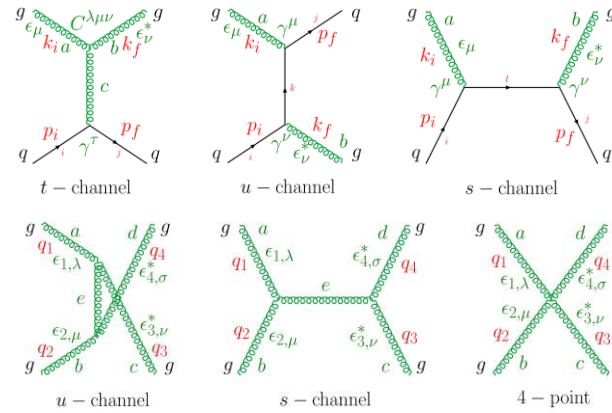


Transport coefficients at finite μ_B

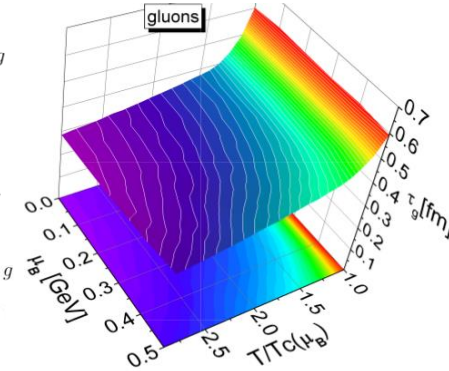
$$\eta^{\text{RTA}}(T, \mu_B) = \frac{1}{15T} \sum_{i=q, \bar{q}, g} \int \frac{d^3p}{(2\pi)^3} \frac{\mathbf{p}^4}{E_i^2} \tau_i(\mathbf{p}, T, \mu_B) d_i(1 \pm f_i) f_i$$

$$\tau_i(\mathbf{p}, T, \mu_B) = \frac{1}{\Gamma_i(\mathbf{p}, T, \mu_B)}$$

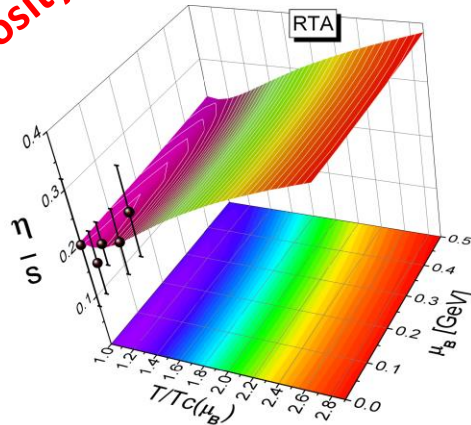
2 \leftrightarrow 2 scatterings



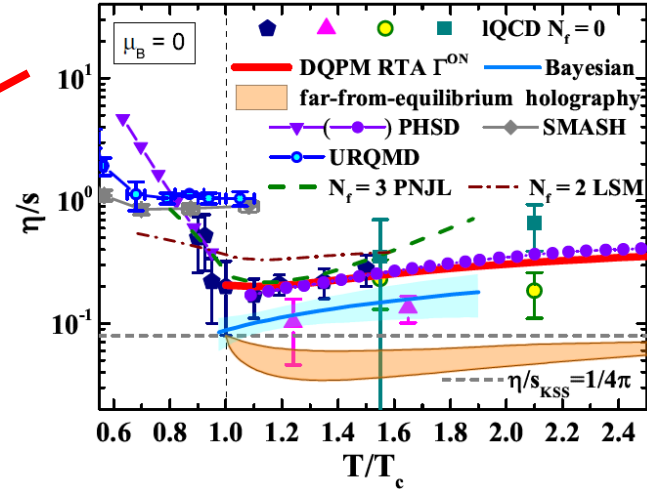
Relaxation times



Specific shear viscosity



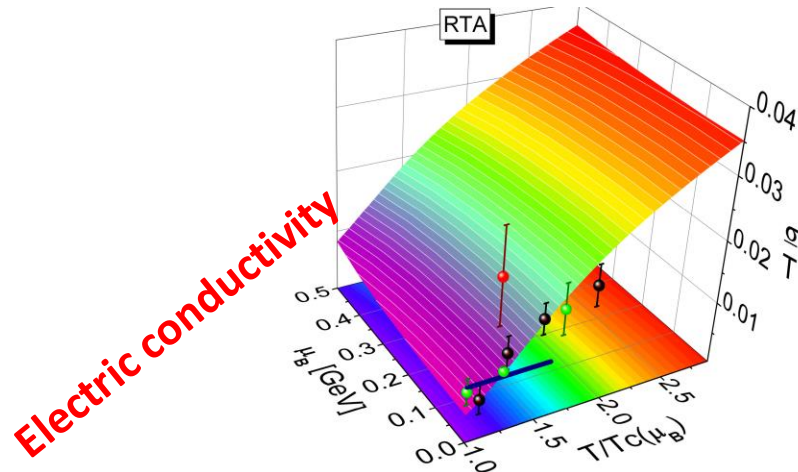
μ_B



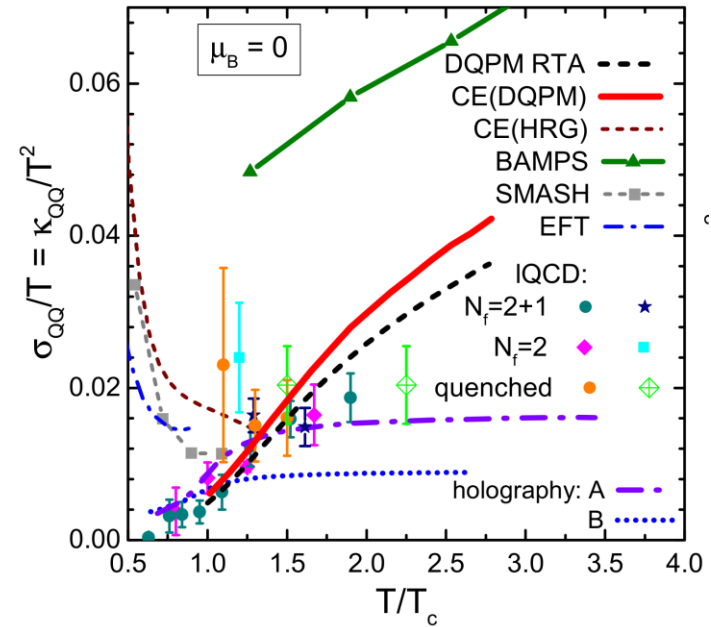
O. S., P. Moreau and E. Bratkovskaya, PRC 101 (2020), 045203

- Good agreement with IQCD predictions and Bayesian estimates
- Light increase with μ_B in the crossover region for viscosities and electric conductivity

Transport coefficients at finite μ_B



μ_B

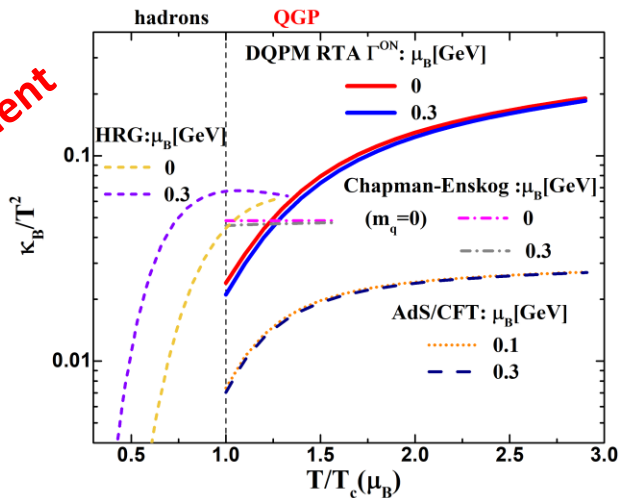


+ Full diffusion coefficient matrix
 has been evaluated $\sigma_q = \kappa_q/T$

$$\begin{pmatrix} j_B^\mu \\ j_Q^\mu \\ j_S^\mu \end{pmatrix} = \begin{pmatrix} \kappa_{BB} & \kappa_{BQ} & \kappa_{BS} \\ \kappa_{QB} & \kappa_{QQ} & \kappa_{QS} \\ \kappa_{SB} & \kappa_{SQ} & \kappa_{SS} \end{pmatrix} \cdot \begin{pmatrix} \nabla^\mu \alpha_B \\ \nabla^\mu \alpha_Q \\ \nabla^\mu \alpha_S \end{pmatrix}$$

J. A. Fotakis, O. S., C. Greiner, O. Kaczmarek and E. Bratkovskaya PRD 104 (2021) , 034014

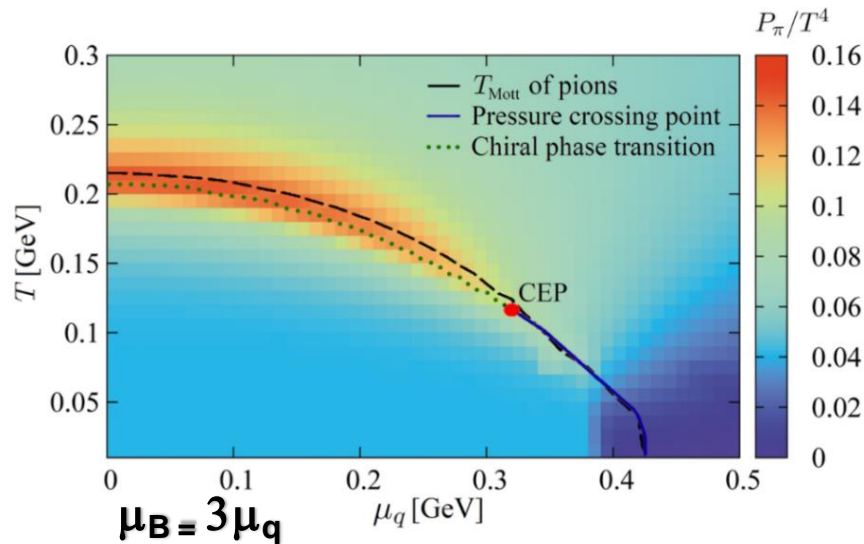
Baryon diffusion coefficient



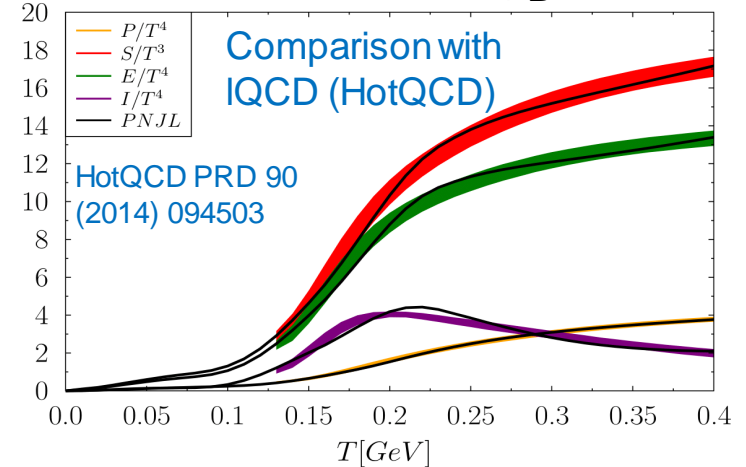
- Light increase with μ_B in the crossover region for shear and bulk viscosities and electric conductivity
- Baryon diffusion coefficients decrease with μ_B

QGP in the Polyakov extended NJL model

- PNJL allows for prediction of macroscopic properties of QGP at finite T and μ_B
- & QGP transport coefficients for $0 \leq \mu_B \leq 1.2$ GeV



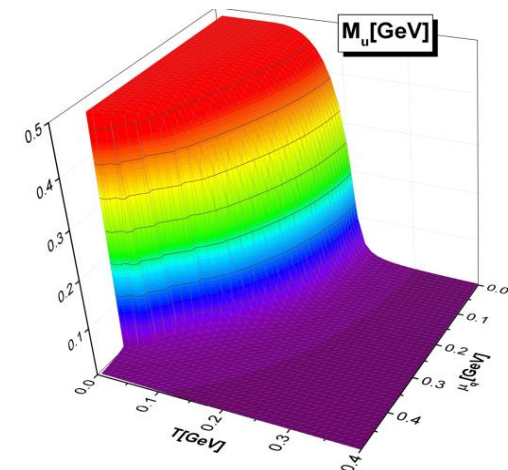
➤ Parameters fixed, EoS at $\mu_B = 0$:



- **CEP**: $(T, \mu_B) = (110, 960)$ MeV, $\mu_B/T = 8.73$
- 1st order PT at high μ_B
- **same symmetries** for the quarks as QCD

Chiral masses (M_l, M_s)

$$m_i = m_{0i} - 4G \langle \langle \bar{\psi}_i \psi_i \rangle \rangle + 2K \langle \langle \bar{\psi}_j \psi_j \rangle \rangle \langle \langle \bar{\psi}_k \psi_k \rangle \rangle$$

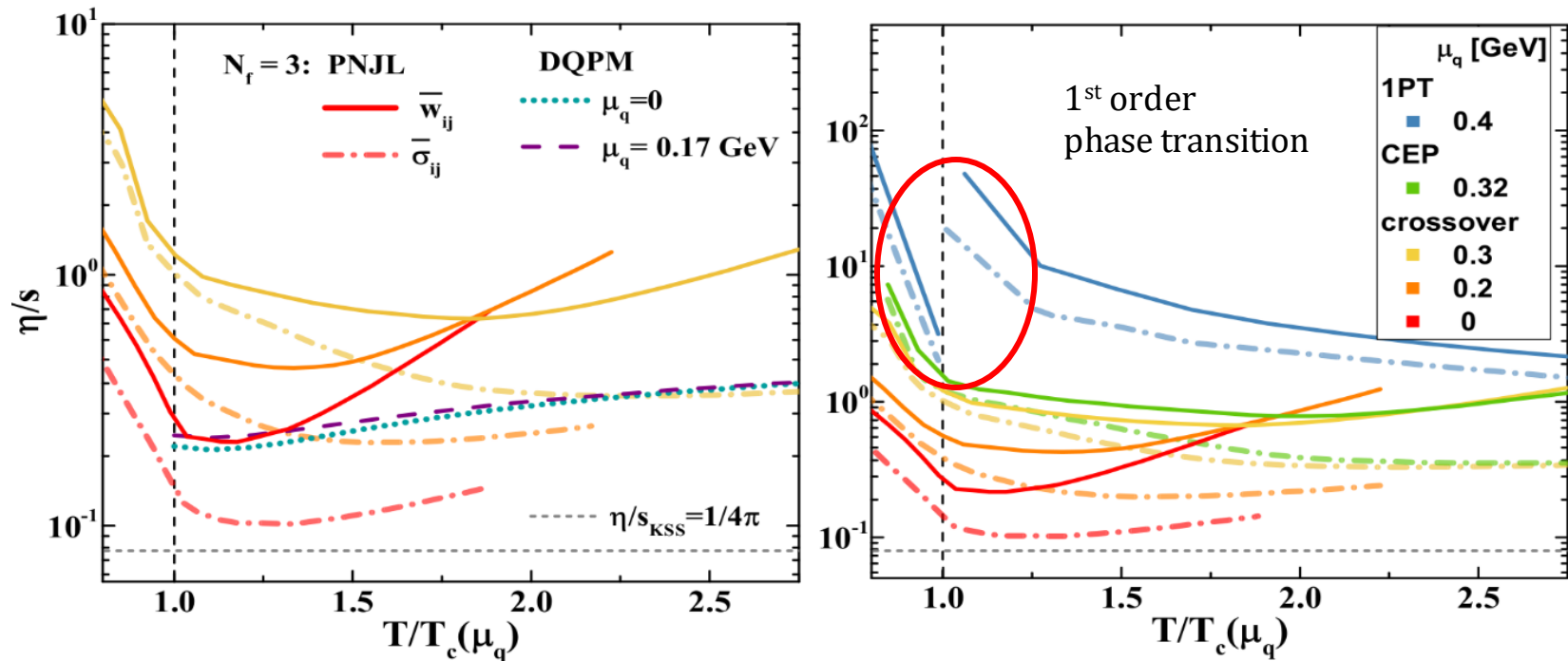


Improved thermodynamics by NNLO in Ω and Polyakov loop

J. M. Torres-Rincon, J. Aichelin PRC 96 (2017) 4 045205

D. Fuseau, T. Steinernert, J. Aichelin PRC 101 (2020) 6 065203

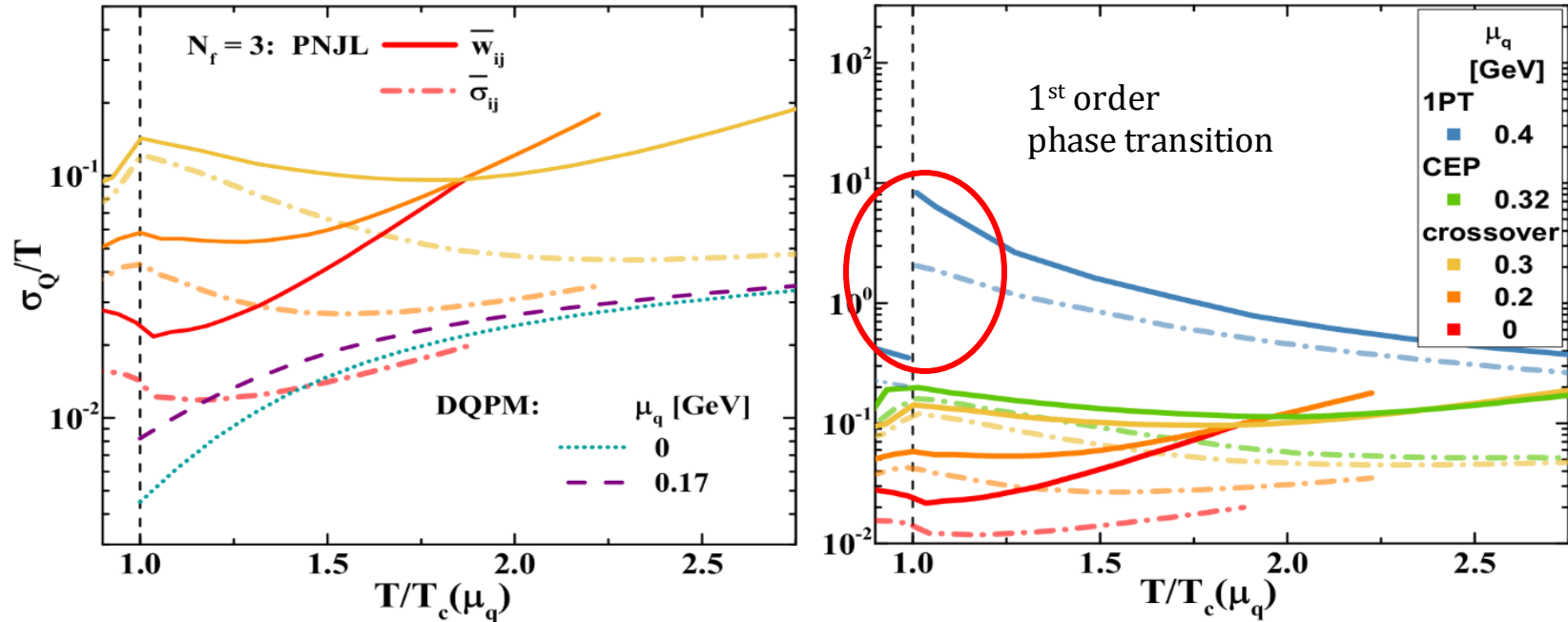
Specific shear viscosity at high μ_B



See also $N_f=2$ NJL results C. Sasaki et al, NPA 832 (2010)

- Two different models have similar increase with μ_B -dependence in the crossover region
- Drastic change of T-dependence for all transport coefficients after 1st order phase transition

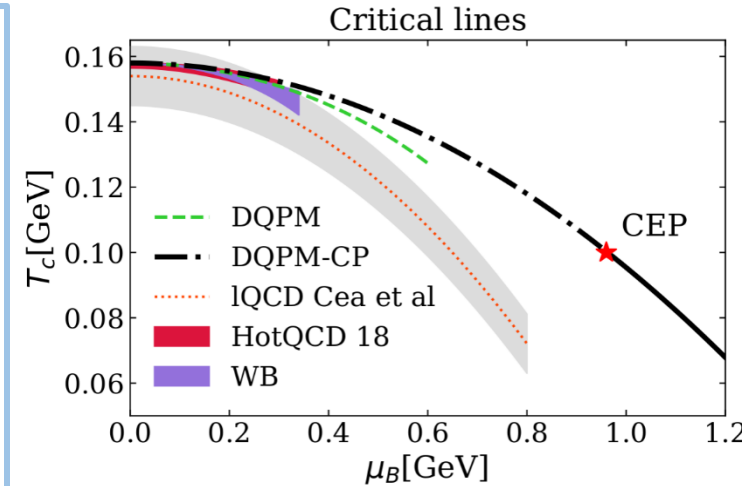
Electric conductivity at high μ_B



- Two different models have similar increase with μ_B -dependence in the crossover region
- Drastic change of T-dependence for all transport coefficients after 1st order phase transition

Quasiparticle model with CEP at high μ_B

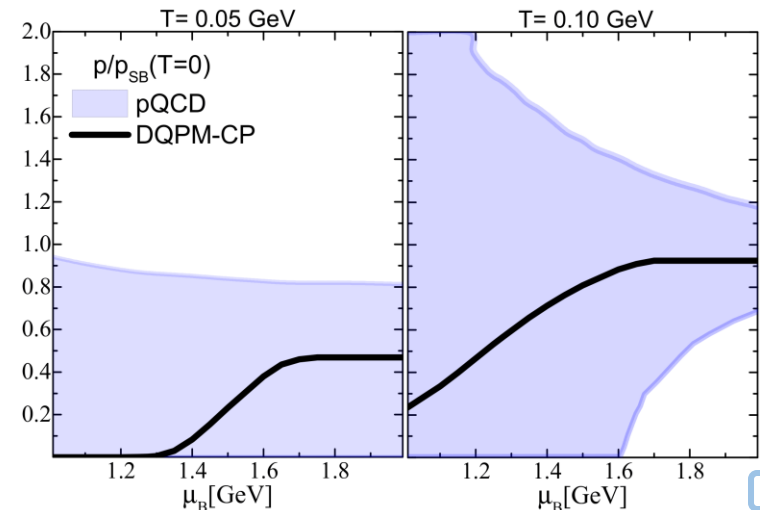
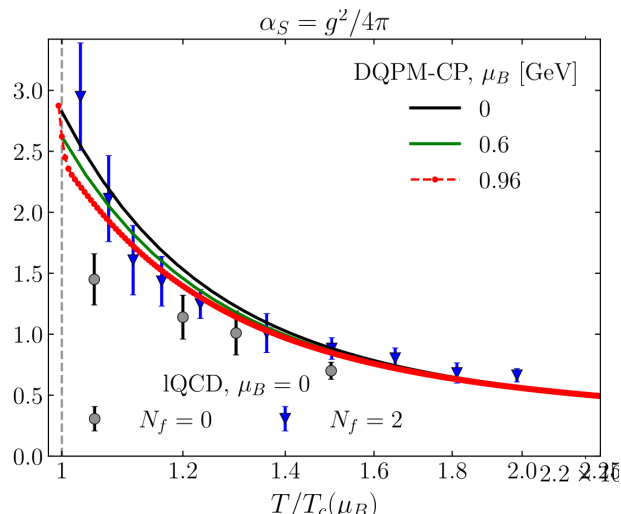
- DQPM-CP for high μ_B , including the CEP region based on the scaling properties of the entropy density from the PNJL model
- DQPM-CP interpolates EoS and microscopic properties between two asymptotics - high $T \gg T_c, \mu_B = 0$ and $T > T_c, \mu_B \gg T$
- EoS and transport coefficients of the QGP phase for the wide range of $T > T_c, \mu_B$



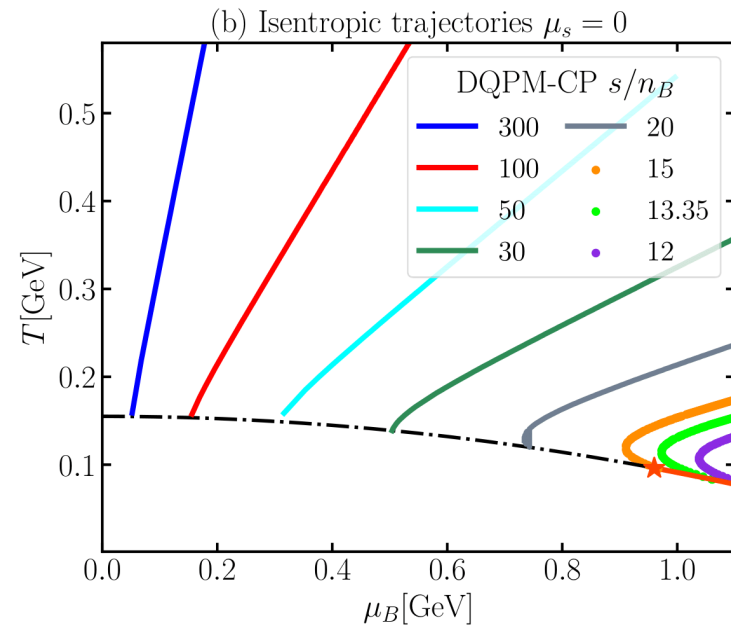
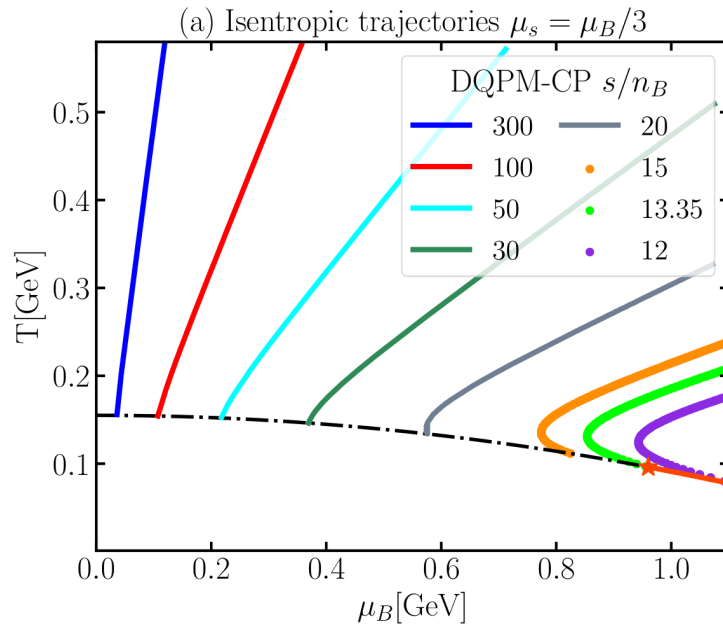
➤ **CEP:** $(T, \mu_B) = (100, 960) \text{ MeV}, \mu_B/T = 9.6$

➤ **EoS:** for $\mu_B/T < 2$ agreement with IQCD for $\mu_B/T > 6$ agreement with pQCD

Near CEP: $g^2 = f(s^{PNJL}(T/T_c)) \rightarrow g^2(T/T_c)$



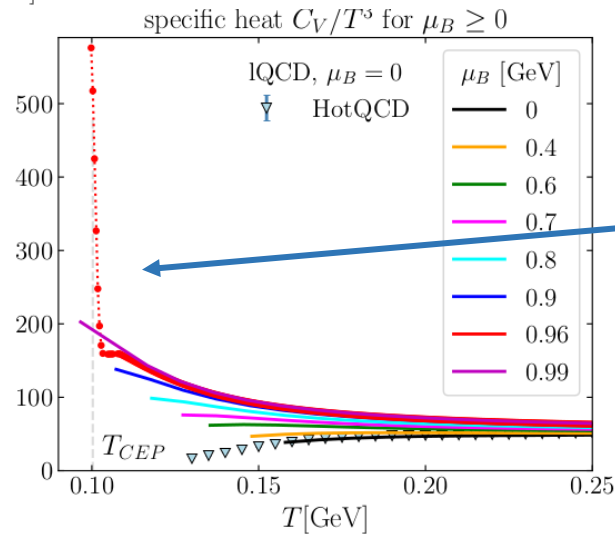
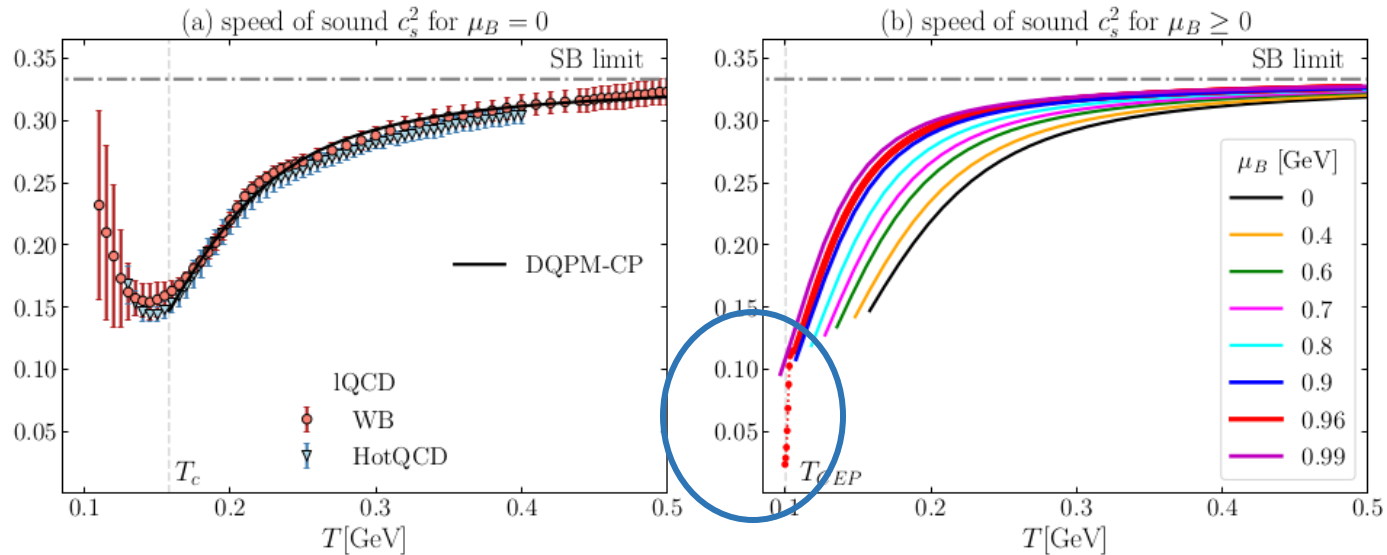
Isentropic trajectories



- CEP acts as an attractor of isentropic trajectories (Chiho Nonaka and Masayuki Asakawa PRC 71 (2005), 044904)
- Trajectories of $s/n_B = \text{const}$ for $\langle ns \rangle = 0$ are shifted towards higher μ_B

Speed of sound

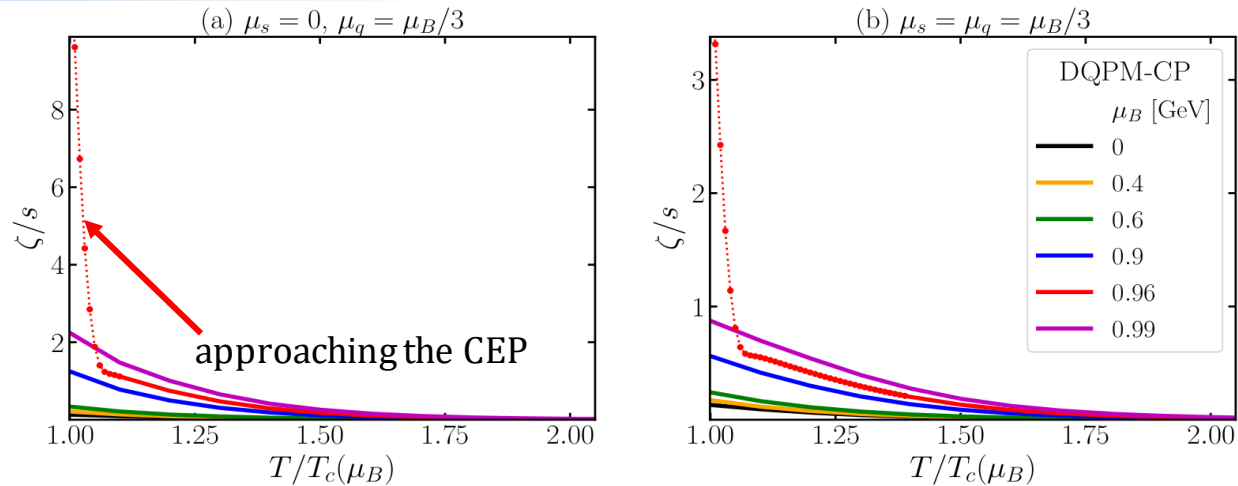
- **EoS** : for $\mu_B/T < 2$ agreement with lQCD for $\mu_B/T > 6$ agreement with pQCD



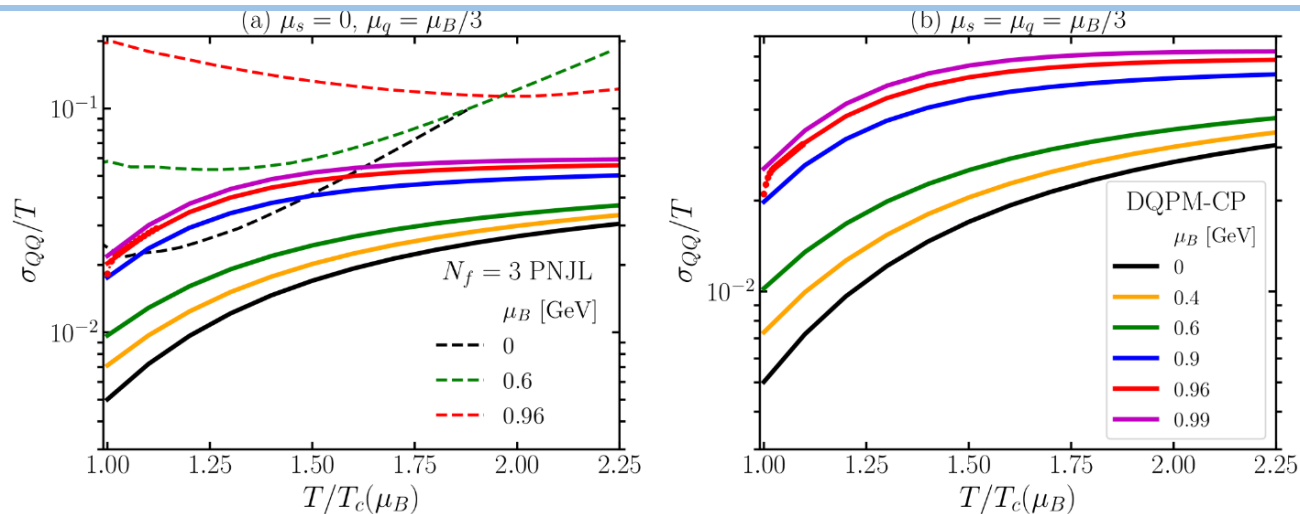
Near CEP critical scaling
can be seen:

$$\ln(C_V) = -\alpha \cdot \ln(T - T_{CEP}) + const$$

Shear and bulk viscosities near the CEP

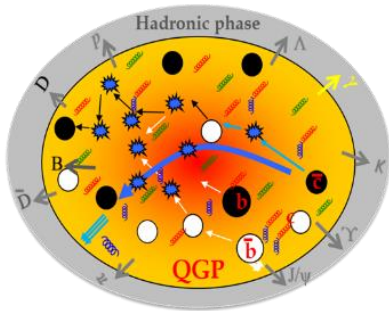


- Sudden rise of specific bulk viscosity approaching the CEP



- B,Q,S diffusion coefficients have pronounced μ_B, μ_S -dependence
- Only small increase approaching the CEP

Modelling HICs: PHSD

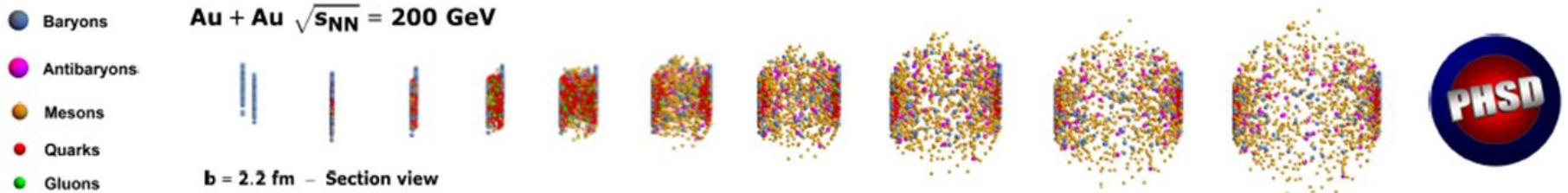


QGP out-of equilibrium \leftrightarrow HIC

Parton-Hadron-String-Dynamics (PHSD)

Non-equilibrium **microscopic transport approach** for the description of strongly-interacting **hadronic** and **partonic** matter created in heavy-ion collisions

Dynamics: based on the solution of generalized off-shell transport equations derived from Kadanoff-Baym many-body theory



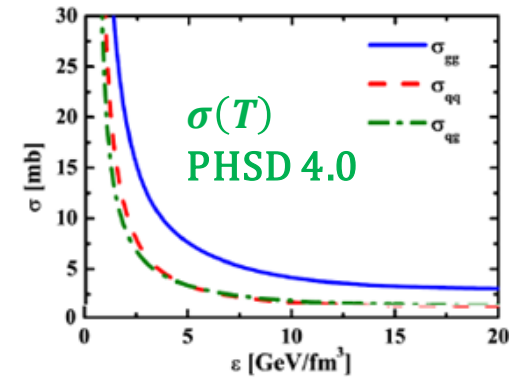
W. Cassing, E. Bratkovskaya, PRC 78 (2008) 034919; NPA831 (2009) 215; W. Cassing, EPJ ST 168 (2009) 3;;
P. Moreau, O. Soloveva, L. Oliva, T. Song, W. Cassing, E. Bratkovskaya, PRC 100 (2019), 014911;
O. Soloveva, P. Moreau, L. Oliva, V. Voronyuk, V. Kireyeu, T. Song, E. Bratkovskaya, Particles 3 (2020), 178-192;....

PHSD

➤ PHSD 4.0 : only isotropic $\sigma(T)$ and $\rho(T)$

parton cross sections

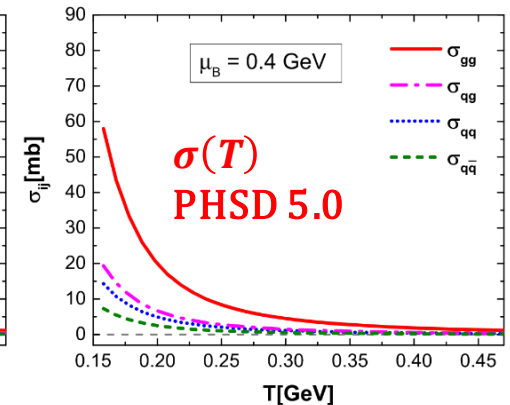
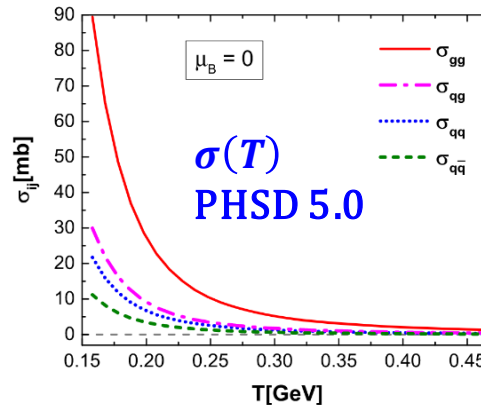
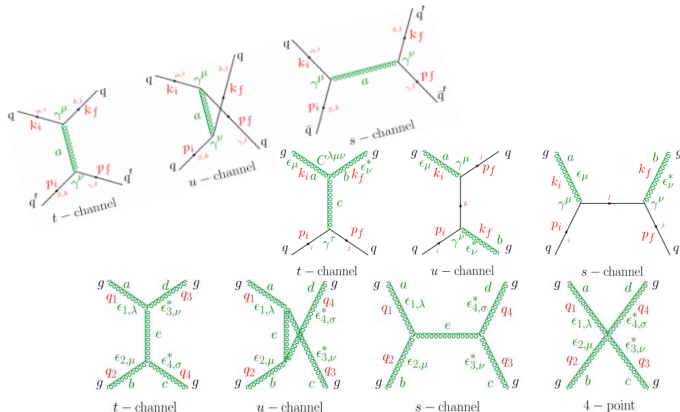
parton spectral function (masses and widths)



new PHSD 5 : angular dependence of $d\sigma/d\cos\theta$

➤ PHSD 5.0 : with $\sigma(\sqrt{s}, m_1, m_2, T, \mu_B = 0)$ and $\rho(T, \mu_B = 0)$

➤ PHSD 5.0 : with $\sigma(\sqrt{s}, m_1, m_2, T, \mu_B)$ and $\rho(T, \mu_B)$



PHSD: extraction of T and μ_B

For each space-time cell of the PHSD: $T^{\mu\nu} = \sum_i \frac{p_i^\mu p_i^\nu}{E_i} \rightarrow$ Diagonalize in LRF $\rightarrow \varepsilon^{\text{PHSD}}$

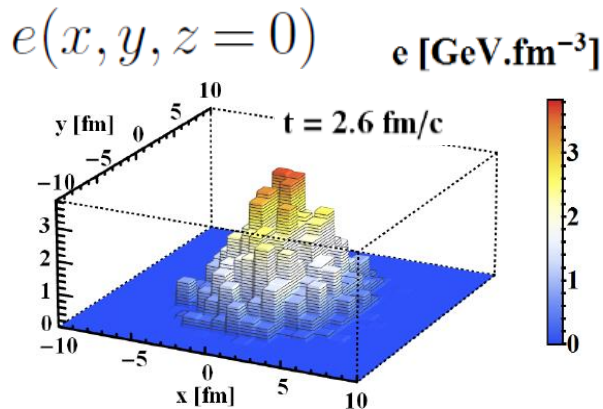
1. Calculate the local energy density $\varepsilon^{\text{PHSD}}$ and baryon density n_B^{PHSD}

2. use IQCD relations
(up to 6th order):

$$\left\{ \begin{array}{l} \frac{n_B}{T^3} \approx \chi_2^B(T) \left(\frac{\mu_B}{T} \right) + \dots \\ \Delta\varepsilon/T^4 \approx \frac{1}{2} \left(T \frac{\partial \chi_2^B(T)}{\partial T} + 3\chi_2^B(T) \right) \left(\frac{\mu_B}{T} \right)^2 + \dots \end{array} \right.$$

Use baryon number susceptibilities χ_n from IQCD

Obtain T, μ_B by solving system of coupled eqs using ε, n_B



Input:
 $\varepsilon^{\text{PHSD}}$ and n_B^{PHSD}



Output:
 T, μ_B

for details see P. Moreau, O. S., L. Oliva, T. Song, W. Cassing, E. Bratkovskaya
arXiv:1903.10157, PRC 100 (2019) no. 1, 014911

PHSD: QGP evolution in HICs

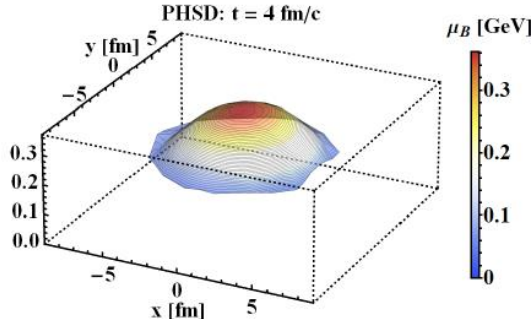
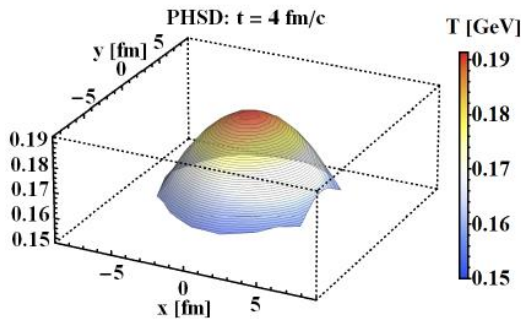
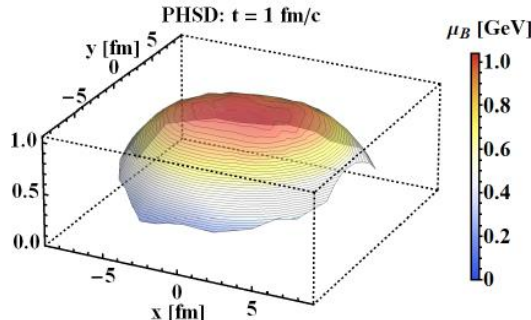
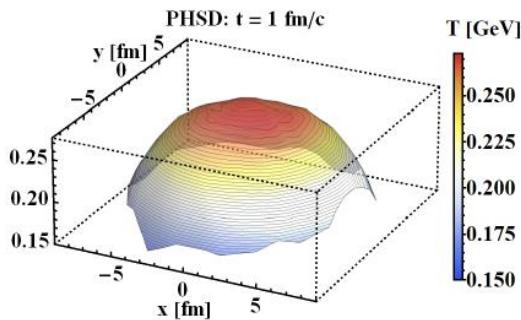
Input:
 ϵ^{PHSD} and n_B^{PHSD}



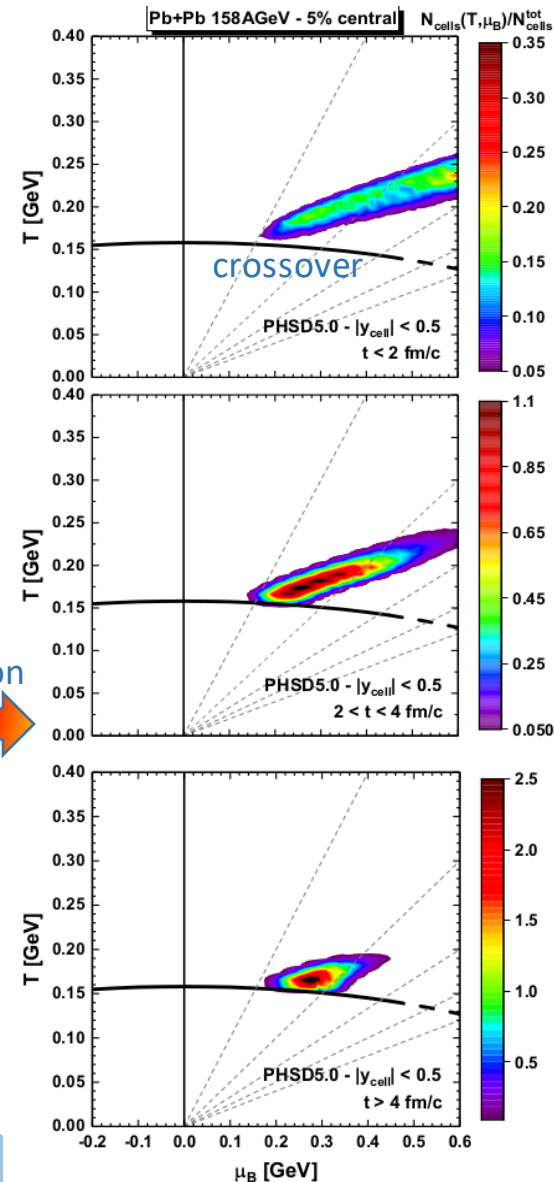
Output:
 T, μ_B

The T -profile in $(x;y)$ & μ_B profile in $(x;y)$
 at midrapidity ($|y_{\text{cell}}| < 1$) at fixed times (1 and 4 fm/c)

Pb+Pb 158A GeV - 5% central



time evolution



Path through the phase diagram is not trivial and localized

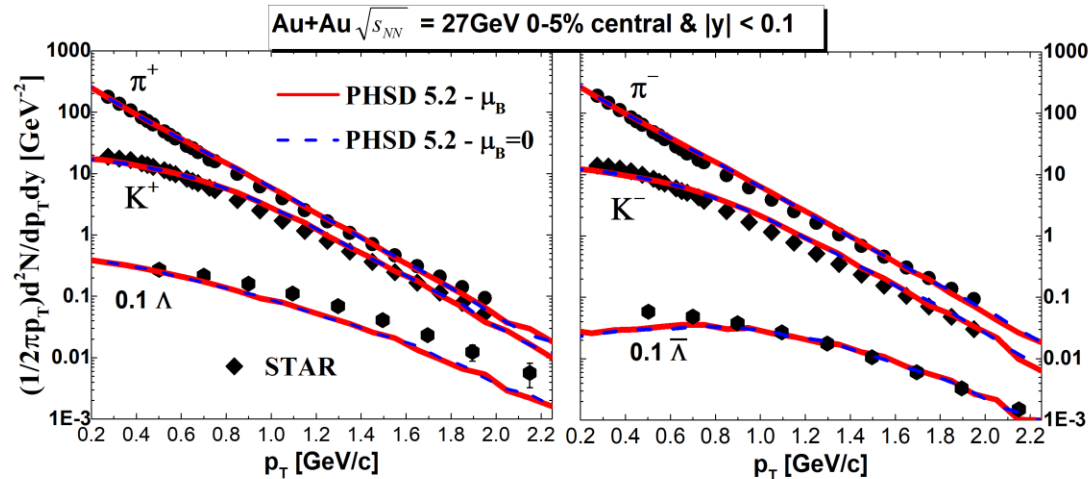
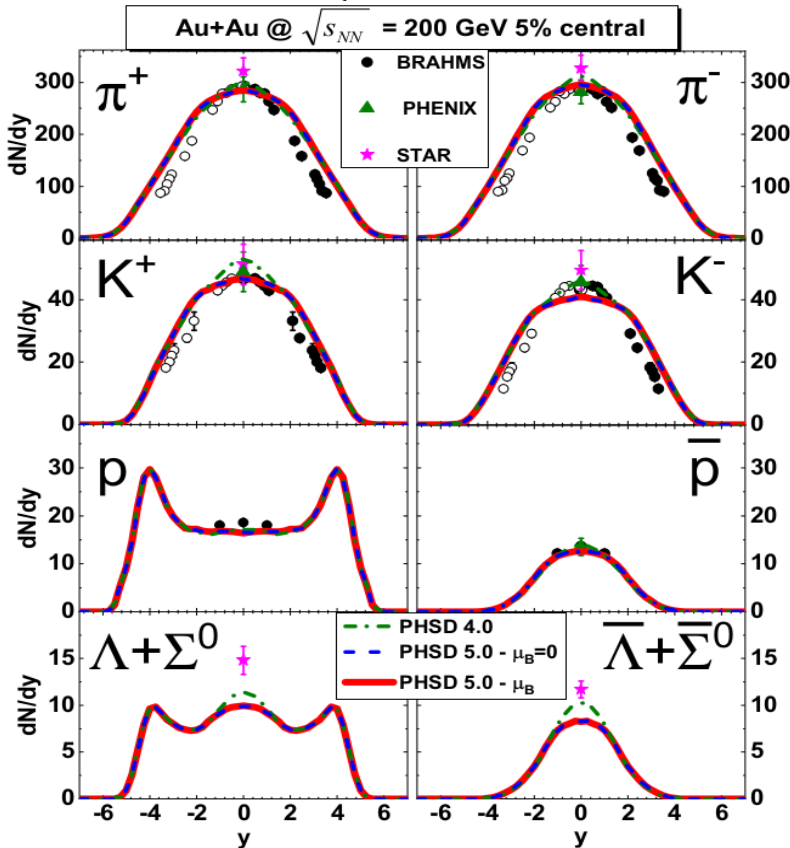
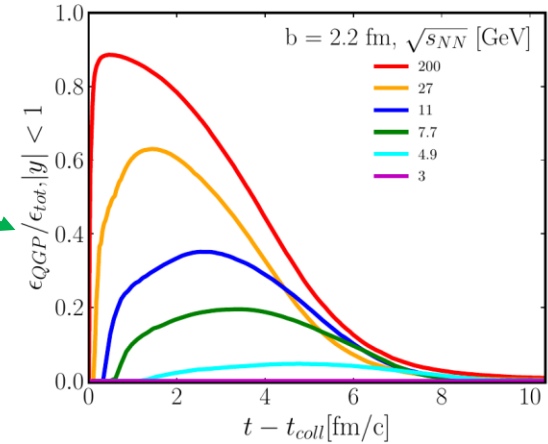
Results for ($\sqrt{s_{NN}} = 200 \text{ GeV} - 7 \text{ GeV}$)



- No visible effects on p_T -spectra, dN/dy of μ_B -dependence
- Small effect of the angular dependence of $d\sigma/d\cos\theta$

at high $\sqrt{s_{NN}}$ - low μ_B

! QGP fraction is **small** at low $\sqrt{s_{NN}}$



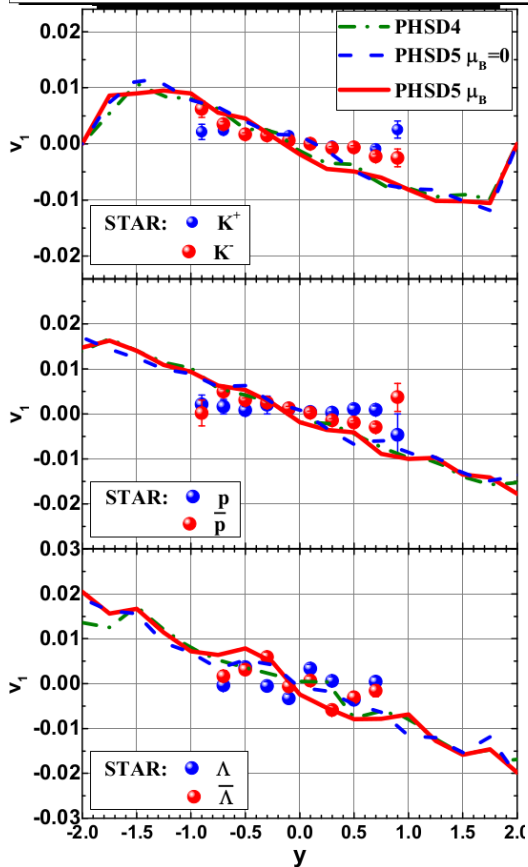
Directed flow ($\sqrt{s_{NN}} = 200 \text{ GeV vs } 27 \text{ GeV}$)

$$v_1 = \left\langle \frac{p_x}{p_T} \right\rangle$$

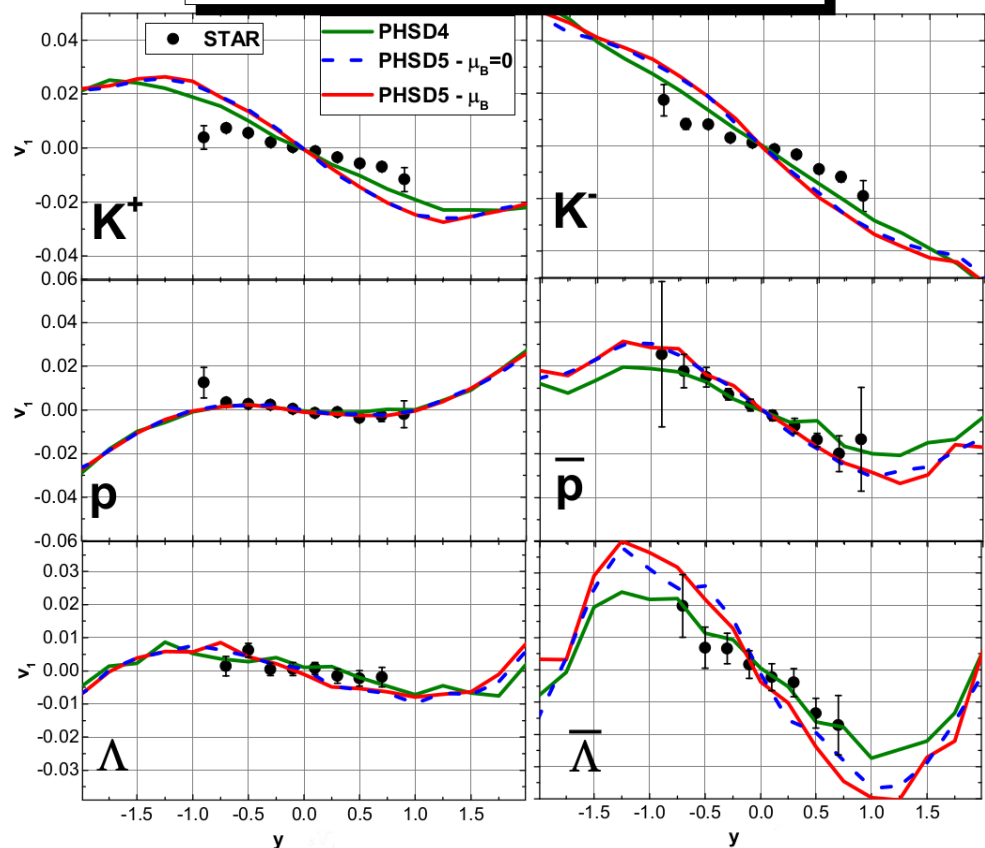
- Influence of the QGP dynamics on final particles observables
- Weak μ_B -dependence – **small** fraction of QGP or **low** μ_B

Particles 3 (2020)
no.1, 178-192

Au+Au $\sqrt{s_{NN}} = 200 \text{ GeV}$ 10-40% centrality



Au+Au $\sqrt{s_{NN}} = 27 \text{ GeV}$ 10-40% centrality

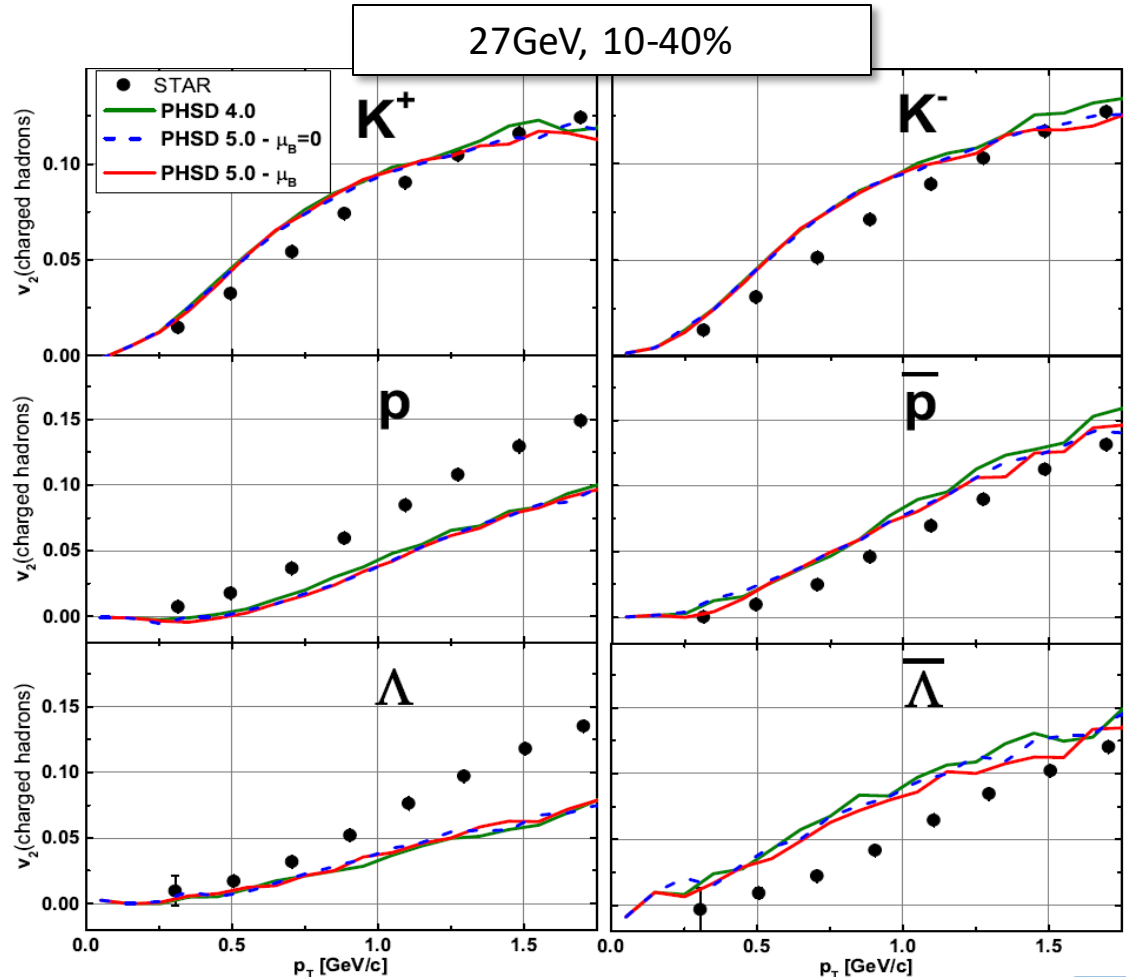
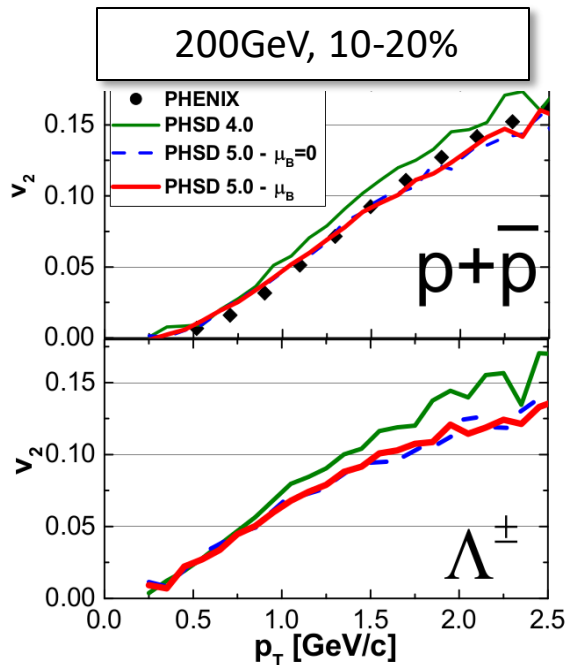


Elliptic flow ($\sqrt{s_{NN}} = 200 \text{ GeV vs } 27 \text{ GeV}$)

$$v_2 = \left\langle \frac{p_x^2 - p_y^2}{p_T^2} \right\rangle$$

- Weak μ_B -dependence
- Small effect of the angular dependence of $d\sigma/d\cos\theta$
- Strong flavor dependence

Particles 3 (2020)
no.1, 178-192



Summary

Transport properties of the strongly-interacting QGP matter at finite T and μ_B have been investigated.

Influence of an order of a phase transition on thermodynamic and transport properties has been studied.

- Transport coefficients can differ among the models, which have similar phase structures and EoS
-

Evolution of the QGP matter created in HICs and the sensitivity of the bulk and flow observables on the QGP interactions and transport properties have been explored by the simulations within the PHSD transport approach

- **High- μ_B** regions are probed at **low $\sqrt{s_{NN}}$** or high rapidity regions
Moreover, **QGP** fraction is **small** at **low $\sqrt{s_{NN}}$** : small effect seen in observables
 - **μ_B -dependence** of QGP interactions is more pronounced in observables for strange hadrons and antiprotons
-

Summary

Transport properties of the strongly-interacting QGP matter at finite T and μ_B have been investigated.

Influence of an order of a phase transition on thermodynamic and transport properties has been studied.

- Transport coefficients can differ among the models, which have similar phase structures and EoS

Evolution of the QGP matter created in HICs and the sensitivity of the bulk and flow observables on the QGP interactions and transport properties have been explored by the simulations within the PHSD transport approach

- **High- μ_B** regions are probed at **low $\sqrt{s_{NN}}$** or high rapidity regions
Moreover, **QGP** fraction is **small** at **low $\sqrt{s_{NN}}$** : small effect seen in observables
- **μ_B -dependence** of QGP interactions is more pronounced in observables for strange hadrons and antiprotons

Outlook:

- 1st/2nd order phase transition in the PHSD
- Possible effects of phase transitions on flow observables

Summary

Transport properties of the strongly-interacting QGP matter at finite T and μ_B have been investigated.

Influence of an order of a phase transition on thermodynamic and transport properties has been studied.

- Transport coefficients can differ among the models, which have similar phase structures and EoS
-

Evolution of the QGP matter created in HICs and the sensitivity of the bulk and flow observables on the QGP interactions and transport properties have been explored by the simulations within the PHSD transport approach

- **High- μ_B** regions are probed at **low $\sqrt{s_{NN}}$** or high rapidity regions
Moreover, **QGP** fraction is **small** at **low $\sqrt{s_{NN}}$** : small effect seen in observables
 - **μ_B -dependence** of QGP interactions is more pronounced in observables for strange hadrons and antiprotons
-

Thank you for your attention!

Back up slides

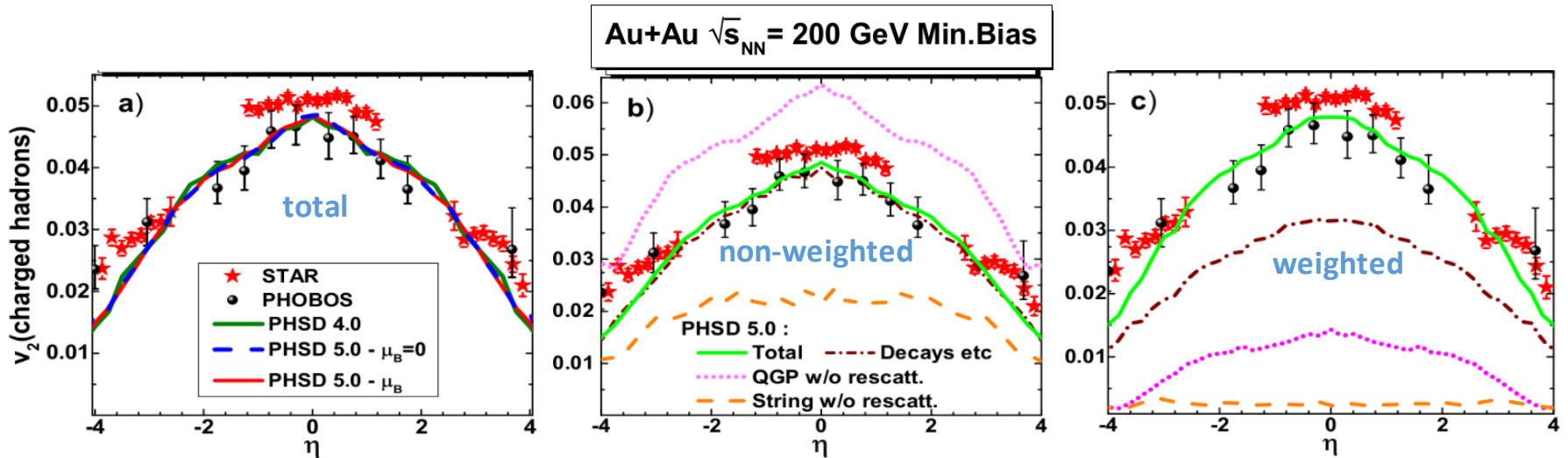
Elliptic flow ($\sqrt{s_{NN}} = 200 \text{ GeV vs } 27 \text{ GeV}$)

$$v_2 = \left\langle \frac{p_x^2 - p_y^2}{p_T^2} \right\rangle$$

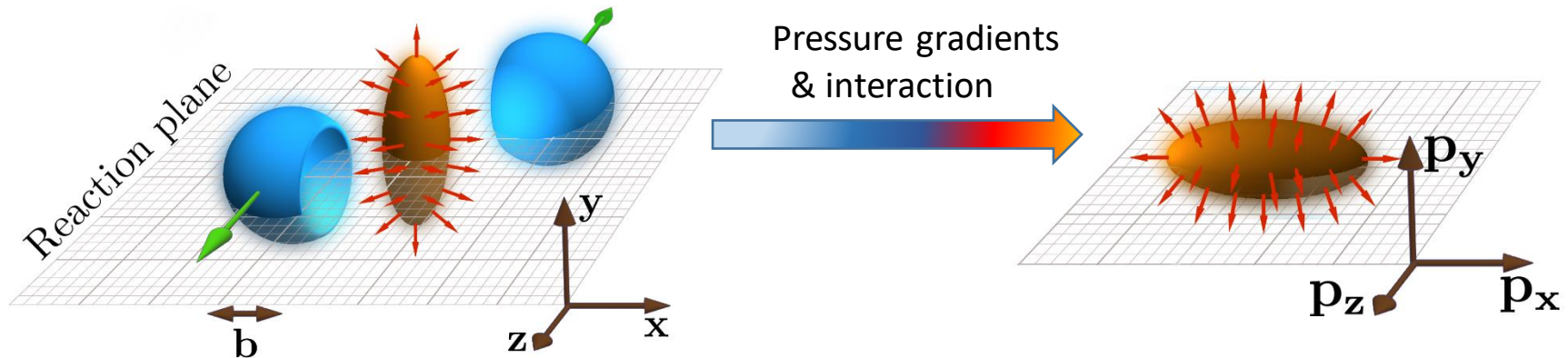
- Weak μ_B -dependence
- Small effect of the angular dependence of $d\sigma/d\cos\theta$
- Strong flavor dependence

Particles 3 (2020)
no.1, 178-192

Channel decomposition :



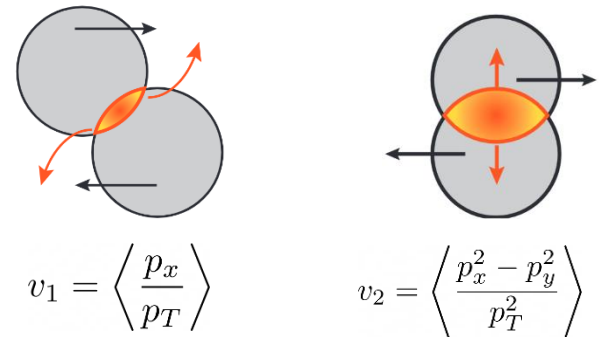
Anisotropic flow coefficients



Quantify the anisotropic flow using Fourier expansion

$$\frac{dN}{d\varphi} \propto \left(1 + 2 \sum_{n=1}^{+\infty} v_n \cos[n(\varphi - \psi_n)] \right)$$

$$v_n = \left\langle \cos n(\varphi - \psi_n) \right\rangle, \quad n = 1, 2, 3, \dots$$

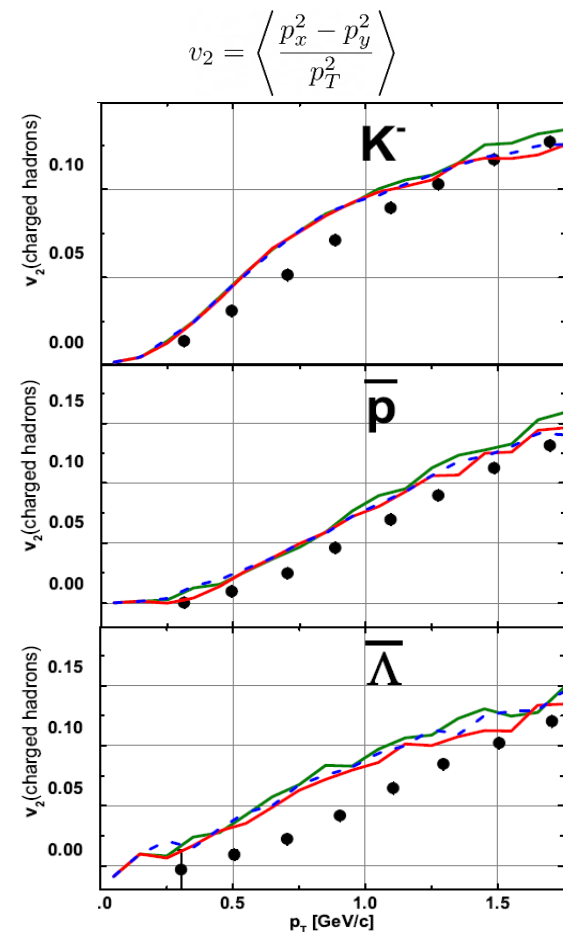
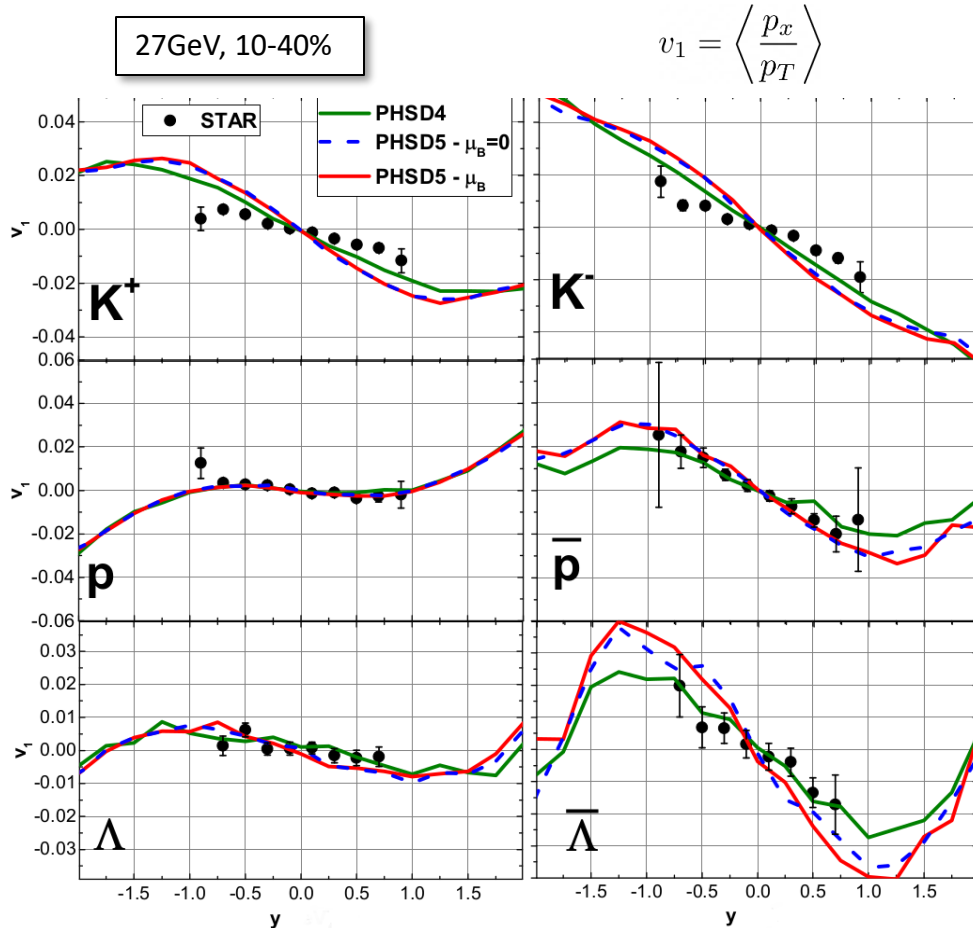


Anisotropic flow

- Assess the transport properties of the QGP
- Sensitive to the QGP EoS and initial state
- Validate models of bulk evolution that are used in the computation of other observables

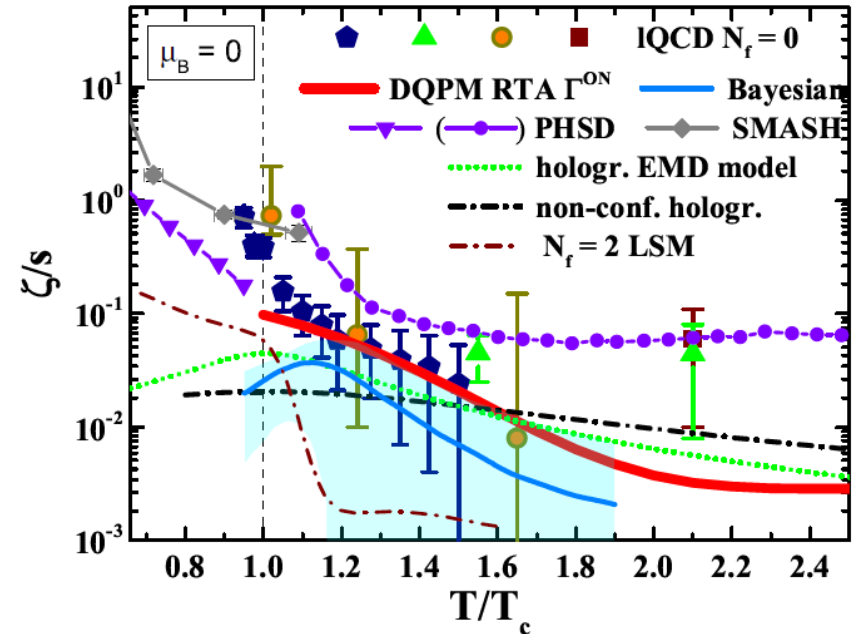
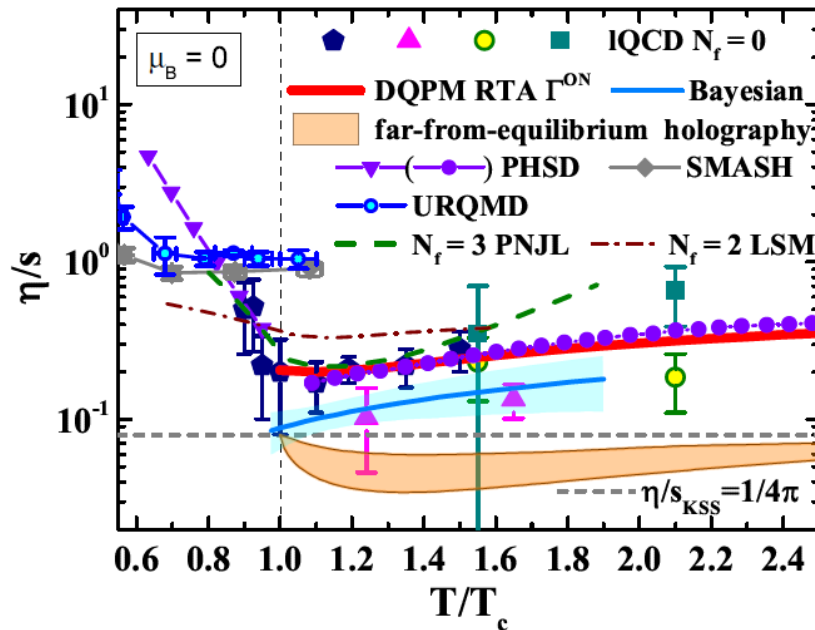
Elliptic flow ($\sqrt{s_{NN}} = 200 \text{ GeV} - 27 \text{ GeV}$)

- Weak μ_B -dependence – small fraction of QGP or low μ_B
- Small effect of the angular dependence of $d\sigma/d\cos\theta$
- Strong flavor dependence



Specific shear viscosity compilation

Model predictions:



! Different models using the same EoS can have completely different transport coefficients!

PNJL relaxation times

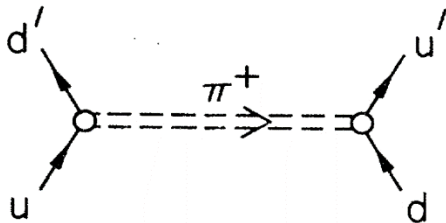
$$\tau_i(\mathbf{p}, T, \mu_B) = \frac{1}{\Gamma_i(\mathbf{p}, T, \mu_B)}$$

$$\Gamma_i^{\text{non}}(\mathbf{p}_i, T, \mu_q) = \frac{1}{2E_i} \sum_{j=q, \bar{q}, g} \int \frac{d^3 p_j}{(2\pi)^3 2E_j} d_j f_j(E_j, T, \mu_q) \int \frac{d^3 p_3}{(2\pi)^3 2E_3} \int \frac{d^3 p_4}{(2\pi)^3 2E_4} (1 \pm f_3)(1 \pm f_4)$$

$$|\bar{\mathcal{M}}|^2(p_i, p_j, p_3, p_4) (2\pi)^4 \delta^{(4)}(p_i + p_j - p_3 - p_4)$$

qq - interactions:

4 point interaction -> meson exchange ($\pi, \sigma, \eta, \eta', K, \dots$ for s, t, u channels)



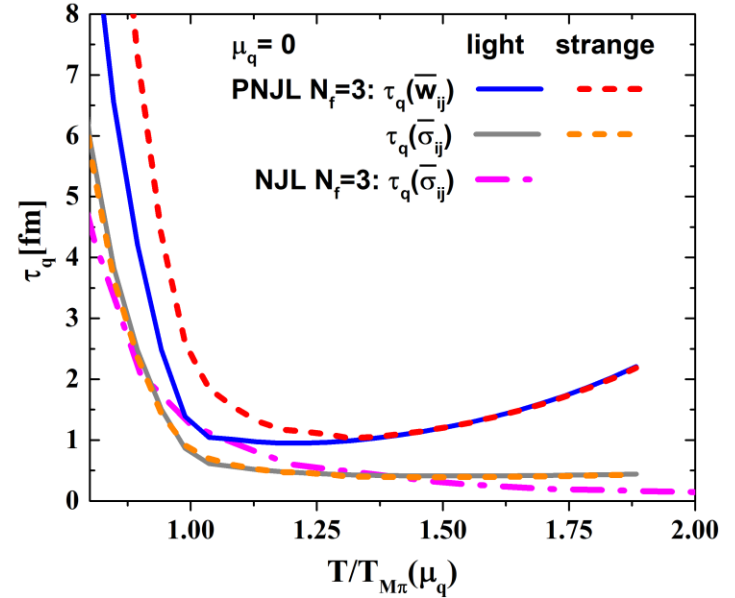
$$\square \text{---} \square \Rightarrow \square \text{---} \square = (i\gamma_5)\tau^{(-)} \frac{-ig_{\pi qq}^2}{k^2 - m_\pi^2} (i\gamma_5)\tau^{(+)}$$

meson propagator $\mathcal{D} = \frac{2ig_m}{1 - 2g_m \Pi_{ff'}^\pm(k_0, \vec{k})}$

Effective interaction in RPA

$$\text{Diagram} \approx \text{Diagram 1} + \text{Diagram 2} + \text{Diagram 3} + \dots = \frac{\text{Diagram 1}}{1 - \text{Diagram 2}}$$

Relaxation times (PNJL vs NJL)



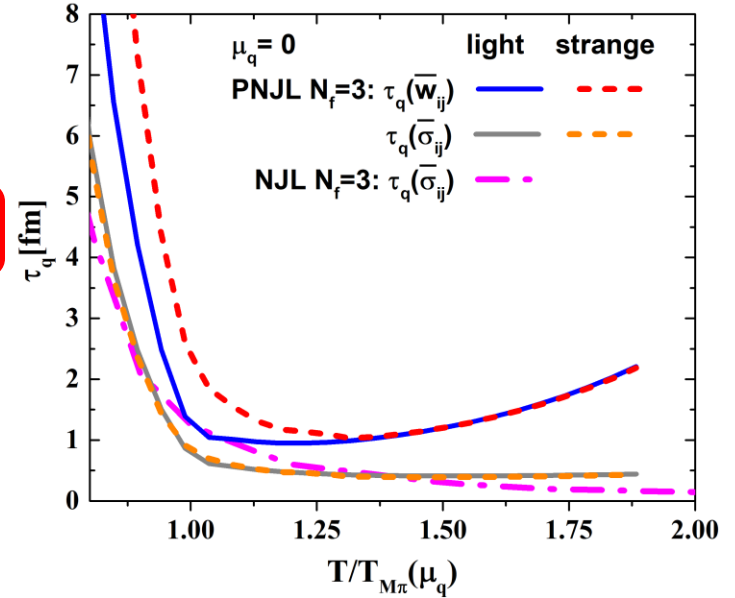
PNJL relaxation times

$$\tau_i(\mathbf{p}, T, \mu_B) = \frac{1}{\Gamma_i(\mathbf{p}, T, \mu_B)}$$

$$\Gamma_i^{\text{on}}(\mathbf{p}_i, T, \mu_q) = \frac{1}{2E_i} \sum_{j=q, \bar{q}, g} \int \frac{d^3 p_j}{(2\pi)^3 2E_j} d_j f_j(E_j, T, \mu_q)$$

$$\int \frac{d^3 p_3}{(2\pi)^3 2E_3} \int \frac{d^3 p_4}{(2\pi)^3 2E_4} (1 \pm f_3)(1 \pm f_4)$$

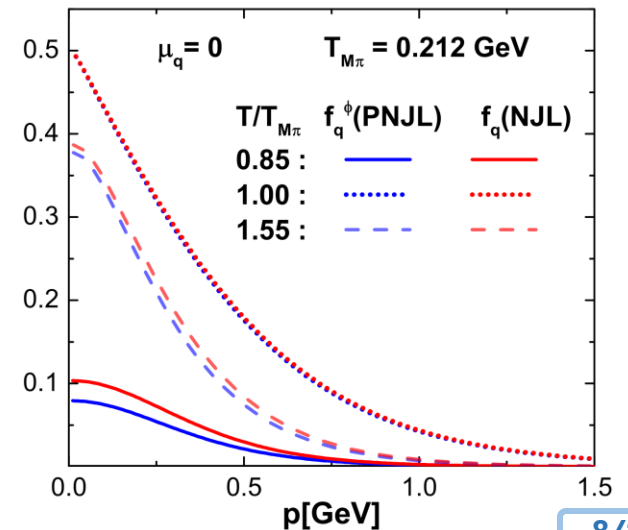
$$|\bar{\mathcal{M}}|^2(p_i, p_j, p_3, p_4) (2\pi)^4 \delta^{(4)}(p_i + p_j - p_3 - p_4)$$



Modified distribution functions:
Polyakov loop contributions

$$f_q \rightarrow f_q^\Phi(\mathbf{p}, T, \mu)$$

$$= \frac{(\bar{\Phi} + 2\Phi e^{-(E_p - \mu)/T}) e^{-(E_p - \mu)/T} + e^{-3(E_p - \mu)/T}}{1 + 3(\bar{\Phi} + \Phi e^{-(E_p - \mu)/T}) e^{-(E_p - \mu)/T} + e^{-3(E_p - \mu)/T}}$$



QGP in the Polyakov extended NJL model

- PNJL model based on effective Lagrangian with the same symmetries for the quark dof as QCD

$$\begin{aligned} \mathcal{L}_{PNJL} = & \sum_i \bar{\psi}_i (iD - m_{0i} + \mu_i \gamma_0) \psi_i \\ & + G \sum_a \sum_{ijkl} \left[(\bar{\psi}_i i\gamma_5 \tau_{ij}^a \psi_j) (\bar{\psi}_k i\gamma_5 \tau_{kl}^a \psi_l) + (\bar{\psi}_i \tau_{ij}^a \psi_j) (\bar{\psi}_k \tau_{kl}^a \psi_l) \right] \\ & - K \det_{ij} \left[\bar{\psi}_i (-\gamma_5) \psi_j \right] - K \det_{ij} \left[\bar{\psi}_i (+\gamma_5) \psi_j \right] \\ & - \mathcal{U}(T; \Phi, \bar{\Phi}) \end{aligned}$$

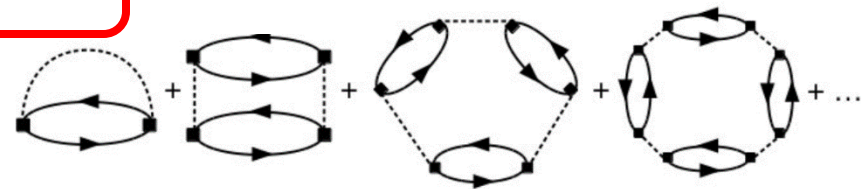
← Polyakov-loop effective potential fitted to the YM

5 parameters fixed by vacuum values K, π masses, η - η' mass splitting, π decay constant, Chiral condensate

Improvements:

- Next to leading order in $N_c (O(1/N_c)^0)$ of the grand-canonical potential : presence of the mesons below T_c

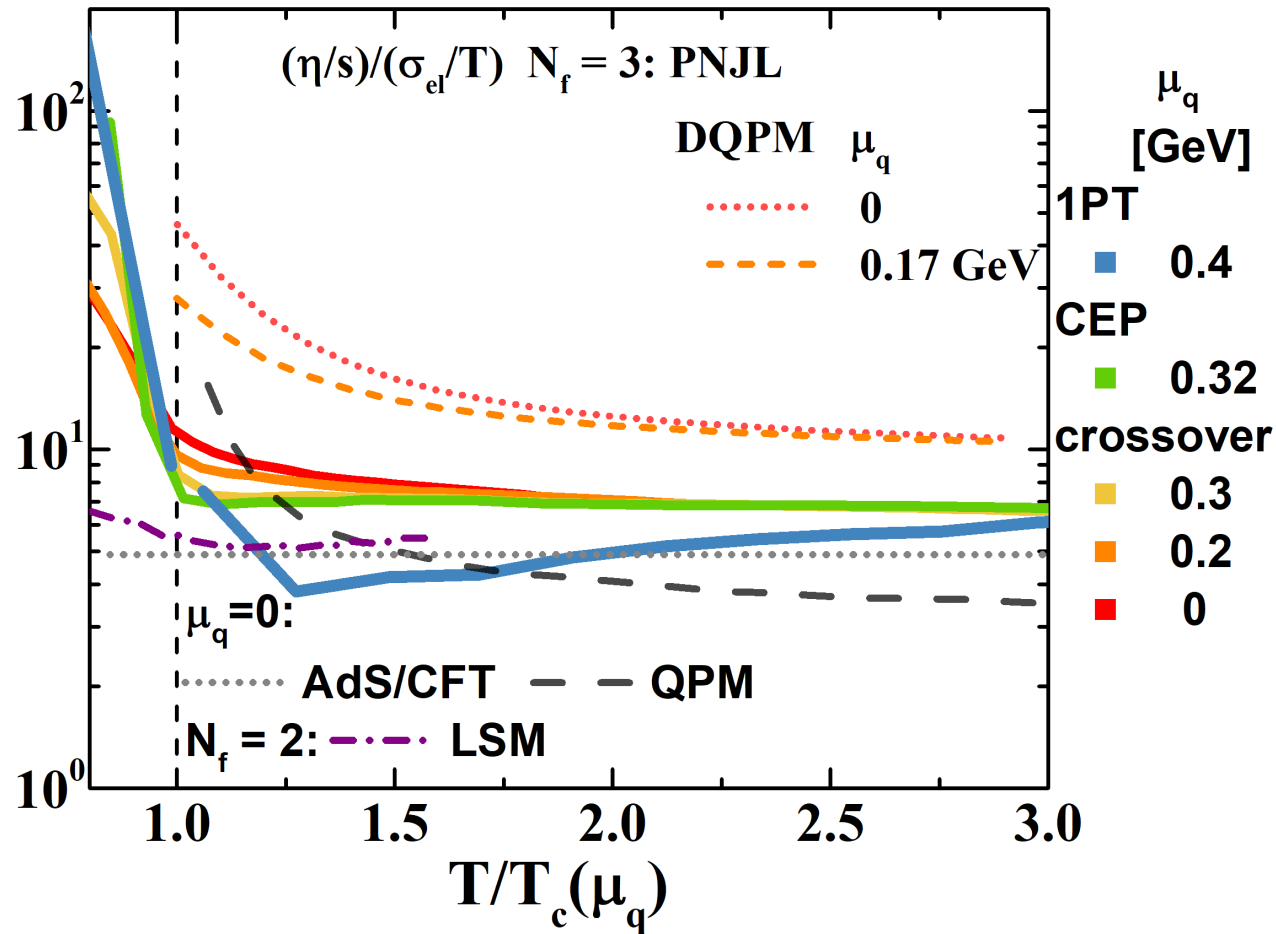
$$\Omega_{PNJL}(T, \mu_i) = \Omega_q^{(-1)}(T, \mu_i) + \sum_{M \in J^\pi = \{0^+, 0^-\}} \Omega_M^{(0)}(T, \mu_M(\mu_i)) + \mathcal{U}_{glue}(T),$$



J. M. Torres-Rincon, J. Aichelin PRC 96 (2017) 4 045205
 D. Fuseau, T. Steinernert, J. Aichelin PRC 101 (2020) 6 065203

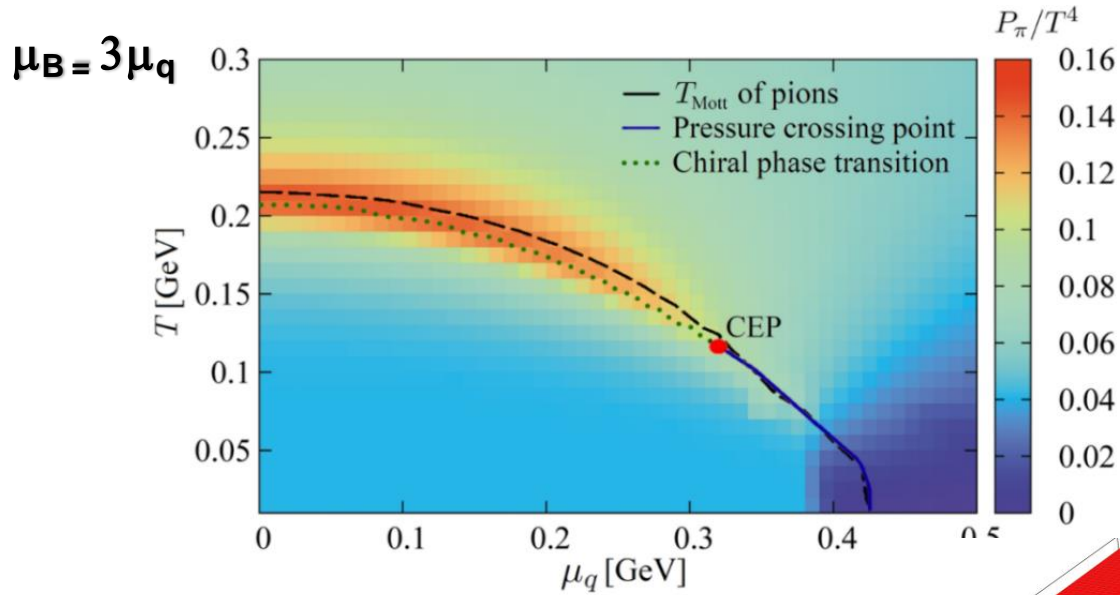
- Modification of the gluon potential due to the presence of the quark

Specific shear viscosity to conductivity



QGP in the Polyakov extended NJL model

- PNJL allows for prediction of macroscopic properties of QGP at finite T and μ_B
- & QGP transport coefficients for $0 \leq \mu_B \leq 1.2$ GeV

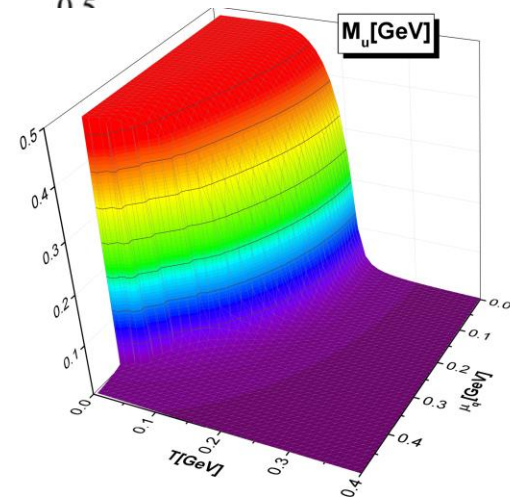


D. Fuseau, T. Steinert, J. Aichelin PRC 101 (2020) 6 065203

- **CEP**: $(T, \mu_B) = (110, 960)$ MeV, $\mu_B/T = 8.73$
- 1st order PT at high μ_B
- **same symmetries** for the quarks as QCD

Chiral masses (M_L, M_S)

$$m_i = m_{0i} - 4G \langle \langle \bar{\psi}_i \psi_i \rangle \rangle + 2K \langle \langle \bar{\psi}_j \psi_j \rangle \rangle \langle \langle \bar{\psi}_k \psi_k \rangle \rangle$$



Specific shear viscosity compilation

- **Kubo formalism: transport coefficients are expressed through correlation functions of stress-energy tensor**

used in lattice QCD, transport approaches(hadrons), effective models

$$\eta = \frac{1}{20} \lim_{\omega \rightarrow 0} \frac{1}{\omega} \int d^4x e^{i\omega t} \langle [S^{ij}(t, \mathbf{x}), S^{ij}(0, \mathbf{0})] \rangle \theta(t) \quad S^{ij} = T^{ij} - \delta^{ij} \mathcal{P}$$

$$\zeta = \frac{1}{2} \lim_{\omega \rightarrow 0} \frac{1}{\omega} \int d^4x e^{i\omega t} \langle [\mathcal{P}(t, \mathbf{x}), \mathcal{P}(0, \mathbf{0})] \rangle \theta(t) \quad \mathcal{P} = -\frac{1}{3} T^i_i$$

R. Lang and W. Weise, EPJ. A 50, 63 (2014) (NJL model)

A. Harutyunyan et al, PRD 95, 114021, (2017)

Kinetic theory:

- **Relaxation time approximation(RTA) : consider relaxation time** $\frac{df_a^{\text{eq}}}{dt} = C_a = -\frac{f_a^{\text{eq}} \phi_a}{\tau_a}$

P. Chakraborty and J. I. Kapusta, PRC 83,014906 (2011)

- **Chapman-Enskog: expand the distribution in terms of the Knudsen number**

J. A. Fotakis et al, PRD 101 (2020) 7, 076007 (HRG)

And more!

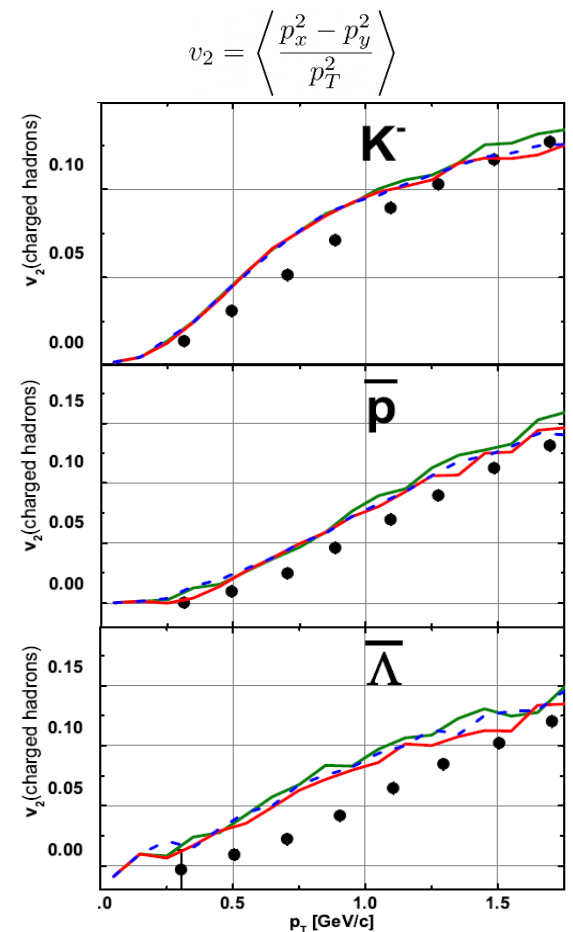
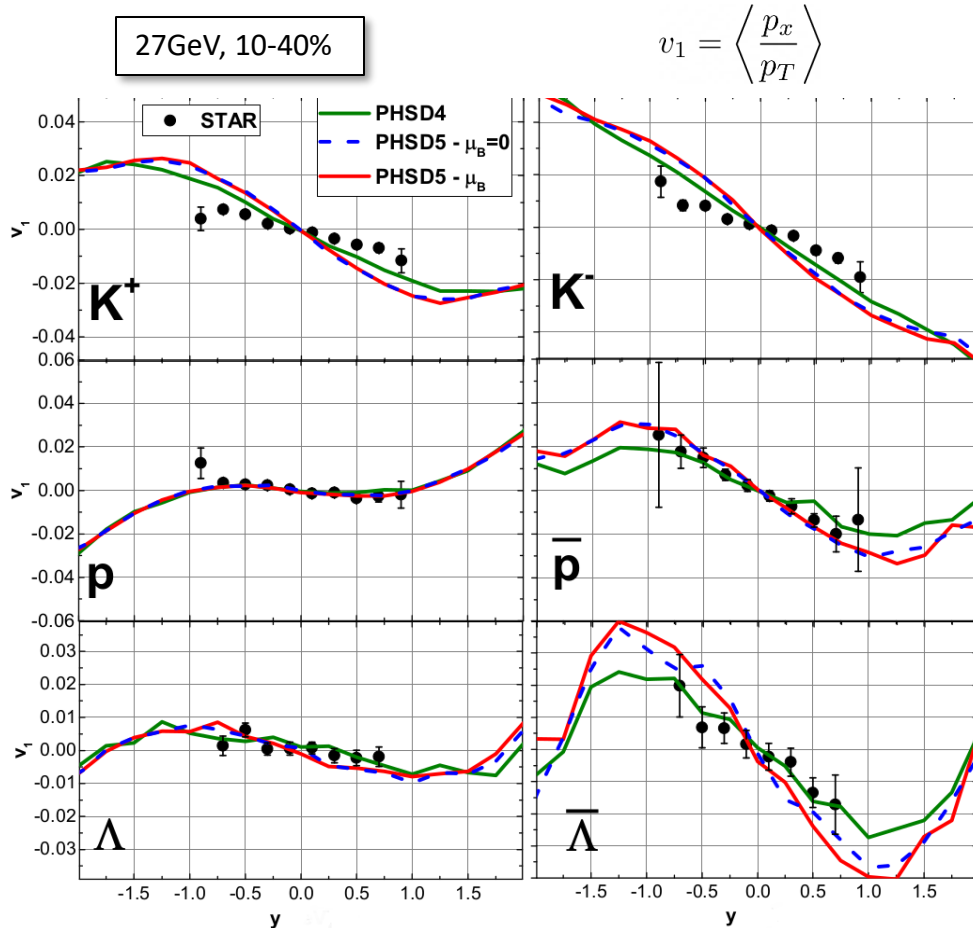
Holographic models: AdS/CFT correspondence

D. T. Son and A. O. Starinets, JHEP 0603, 052 (2006)

M. Attems et al, JHEP 10 (2016), 155.

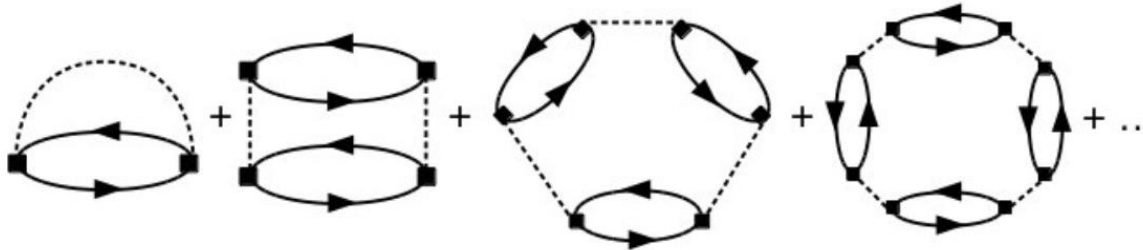
Elliptic flow ($\sqrt{s_{NN}} = 200 \text{ GeV} - 27 \text{ GeV}$)

- Weak μ_B -dependence – small fraction of QGP or low μ_B
- Small effect of the angular dependence of $d\sigma/d\cos\theta$
- Strong flavor dependence



PNJL improvements

- Next to leading order in N_c ($O(1/N_c)^0$) of the grand-canonical potential : **presence of the mesons below T_c**



J. M. Torres-Rincon, J. Aichelin PRC 96 (2017) 4 045205

- **Modification of the gluon potential due to the presence of the quark**

$$\frac{U(\phi, \bar{\phi}, T)}{T^4} = -\frac{b_2(T)}{2} \bar{\phi}\phi - \frac{b_3}{6} (\bar{\phi}^3 + \phi^3) + \frac{b_4}{4} (\bar{\phi}\phi)^2$$

$$b_2(T) = a_0 + \frac{a_1}{1 + \tau} + \frac{a_2}{(1 + \tau)^2} + \frac{a_3}{(1 + \tau)^3} \quad \text{where} \quad \tau_{\text{phen}} = 0.57 \frac{T - T_{\text{phen}}^{\text{cr}}(T)}{T_{\text{phen}}^{\text{cr}}(T)}$$

$$T_{\text{phen}}(T) = a + bT + cT^2 + dT^3 + \boxed{e \frac{1}{T}}$$

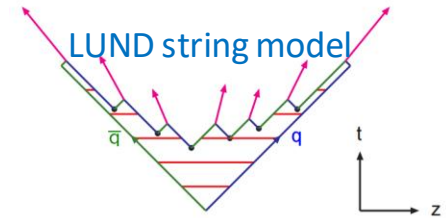
D. Fuseau, T. Steinernert, J. Aichelin PRC 101 (2020) 6 065203

Stages of collisions in PHSD

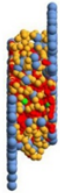
Initial A+A collision



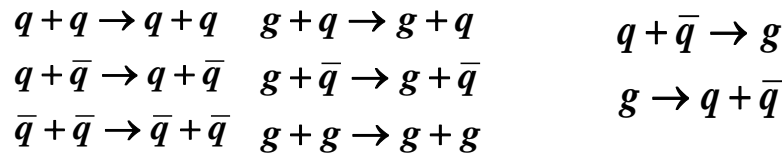
- String formation in primary NN collisions
→ decays to pre-hadrons (baryons and mesons)



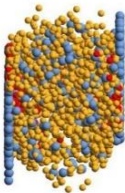
Partonic phase



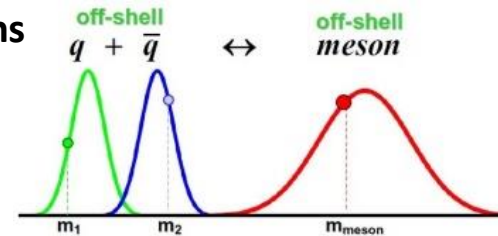
- Formation of a QGP state if $\mathcal{E} > \mathcal{E}_{critical}$:
Dissolution of pre-hadrons → DQPM
→ massive quarks/gluons and mean-field energy
(quasi-)elastic collisions : inelastic collisions:



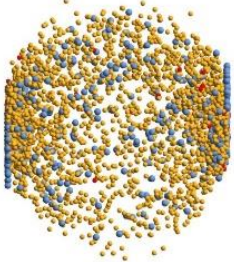
Hadronization



- Hadronization to colorless off-shell mesons and baryons
 $g \rightarrow q + \bar{q}$, $q + \bar{q} \leftrightarrow meson$ ('string')
 $q + q + q \leftrightarrow baryon$ ('string')



Hadronic phase

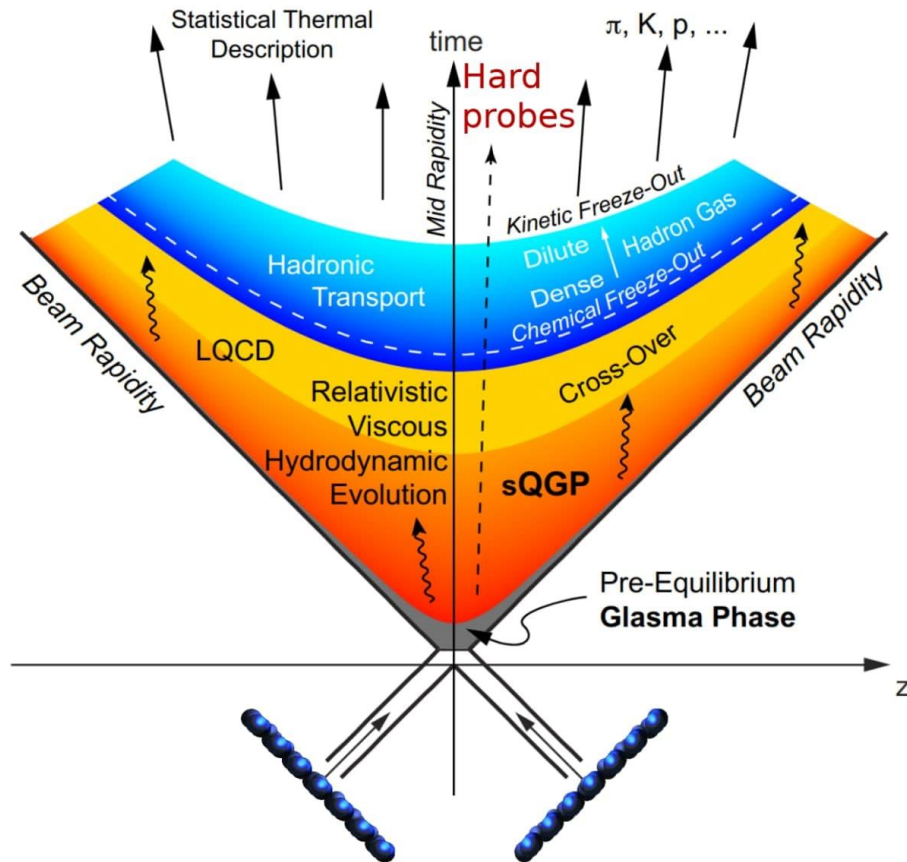


Strict 4-momentum and quantum number conservation

- Hadron-string interactions – off-shell HSD

W. Cassing, E. Bratkovskaya, PRC 78 (2008) 034919; NPA831 (2009) 215;
W. Cassing, EPJ ST 168 (2009) 3

Stages of HIC



$t > 10 \text{ fm}$ - hadronisation and free stream to detectors

$10 \text{ fm} > t > 1 \text{ fm}$ - QGP expansion

$t \approx 1 \text{ fm}$ - Equilibration

$t \ll 1 \text{ fm}$ - Initial state

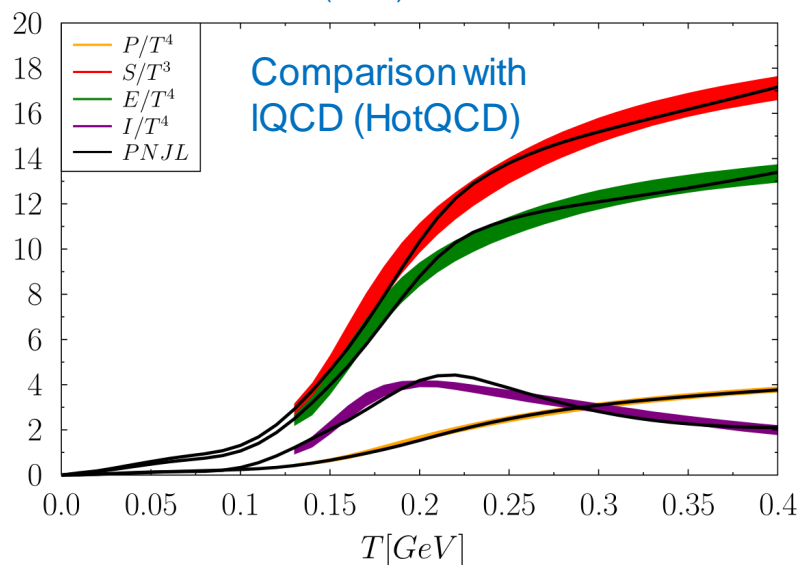
QGP out-of equilibrium \leftrightarrow HIC

QGP in the Polyakov extended NJL model

- PNJL allows for prediction of macroscopic properties of QGP at finite T and μ_B
- & QGP transport coefficients for $0 \leq \mu_B \leq 1.2$ GeV

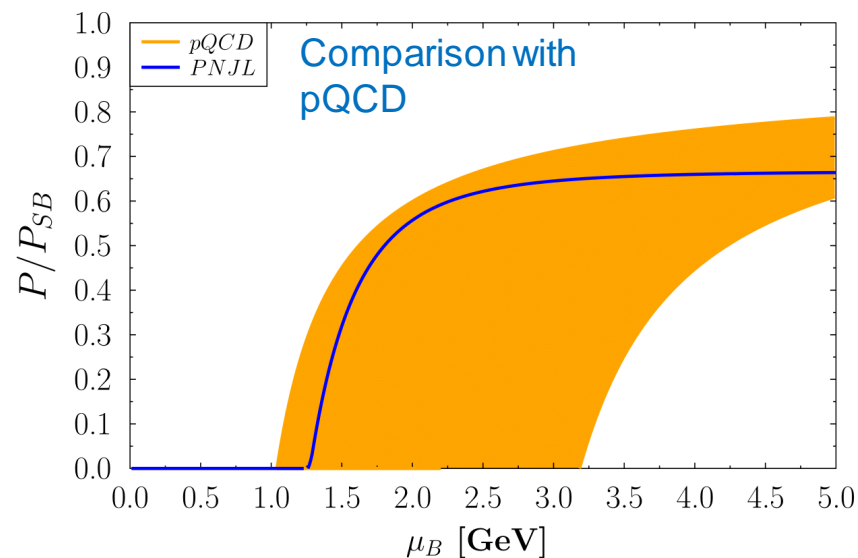
➤ Parameters fixed, EoS at $\mu_B = 0$:

HotQCD PRD 90 (2014) 094503



➤ EoS at high μ_B :

pQCD: A.Kurkela, A.Vuorinen, PRL 117 (2016)4 042501



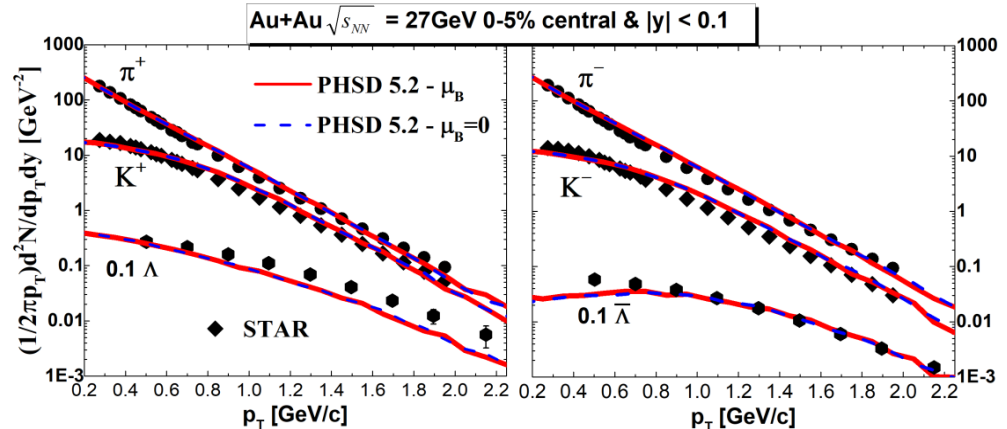
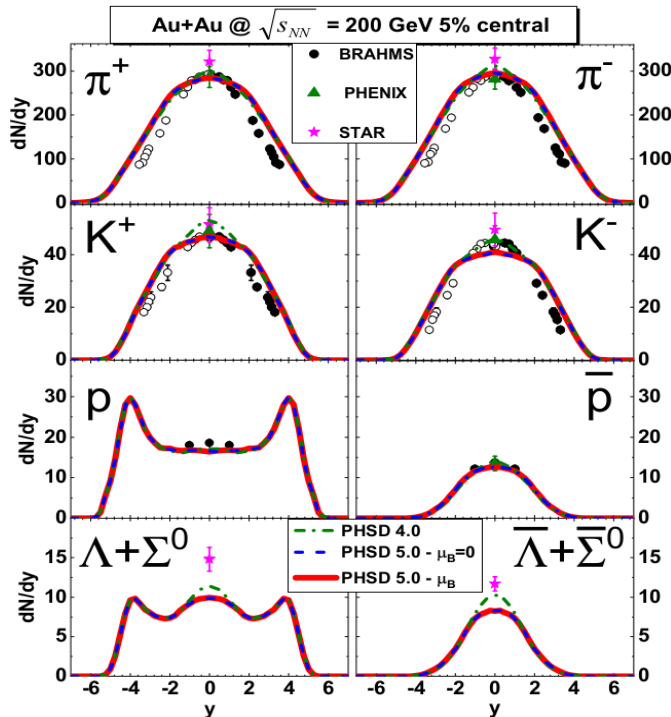
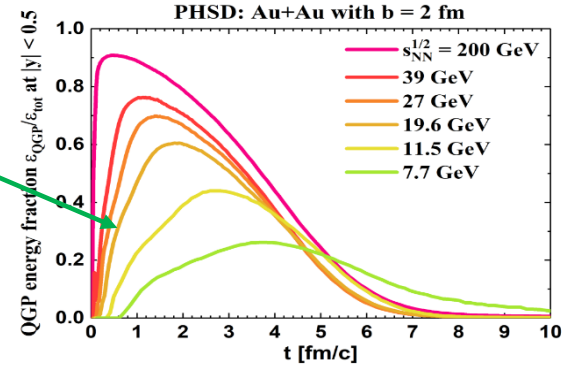
Results for ($\sqrt{s_{NN}} = 200 \text{ GeV} - 7 \text{ GeV}$)



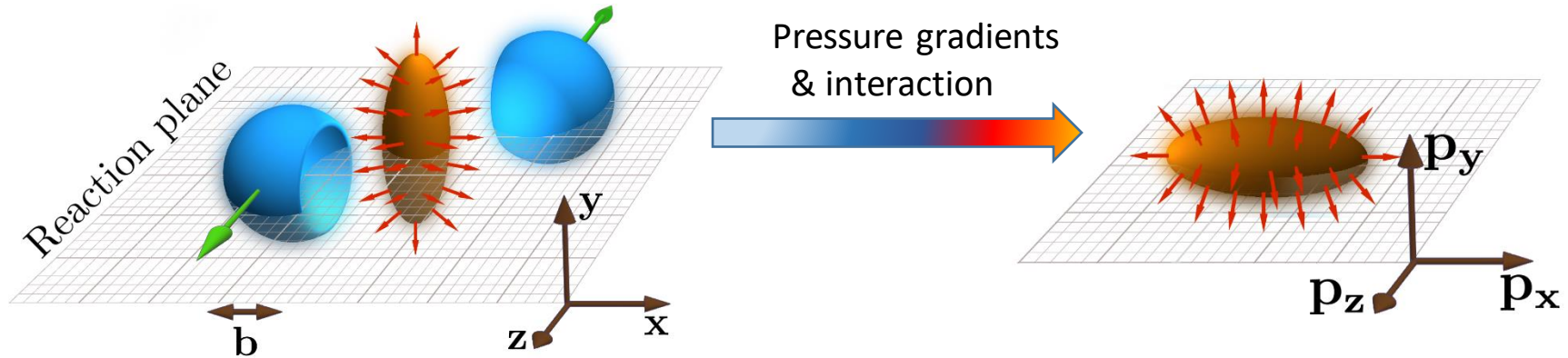
- No visible effects on p_T -spectra, dN/dy of μ_B -dependence
- Small effect of the angular dependence of $d\sigma/d\cos\theta$

at high $\sqrt{s_{NN}}$ - **low** μ_B

! QGP fraction is **small** at low $\sqrt{s_{NN}}$



Anisotropic flow coefficients



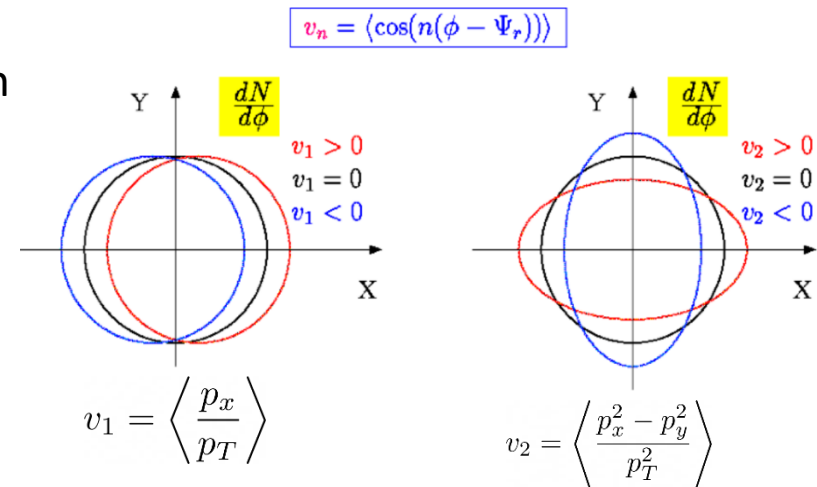
Quantify the anisotropic flow using Fourier expansion

$$\frac{dN}{d\phi} \propto \left(1 + 2 \sum_{n=1}^{+\infty} v_n \cos[n(\phi - \psi_n)] \right)$$

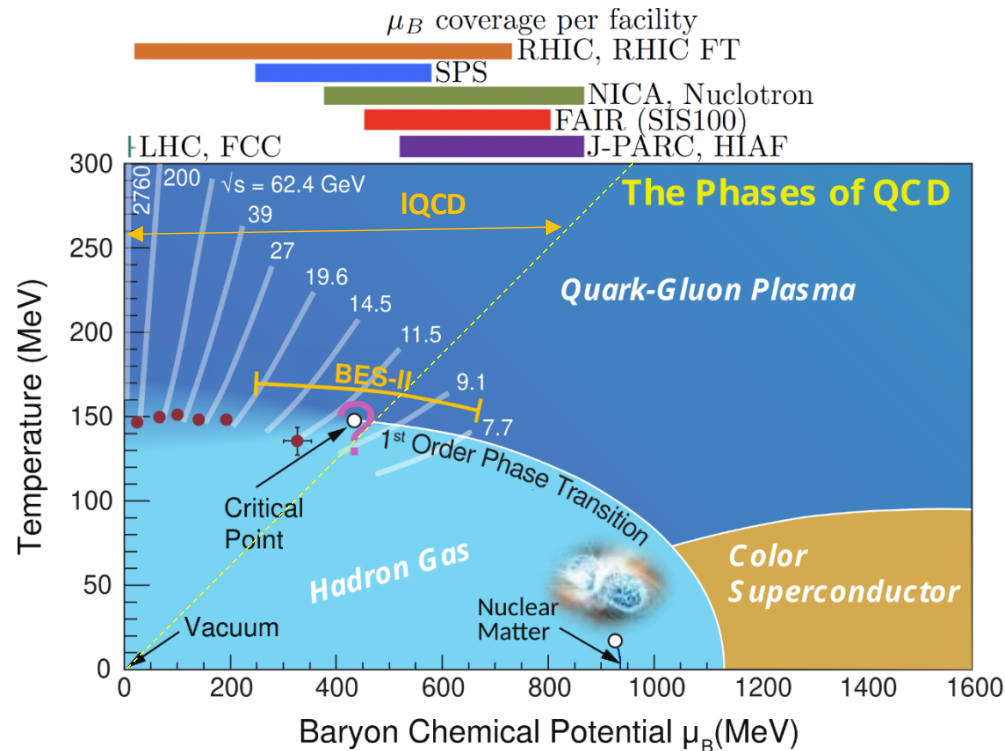
$$v_n = \langle \cos n(\phi - \psi_n) \rangle, \quad n = 1, 2, 3, \dots$$

Anisotropic flow

- Assess the transport properties of the QGP
- Sensitive to the QGP EoS and initial state
- Validate models of bulk evolution that are used in the computation of other observables

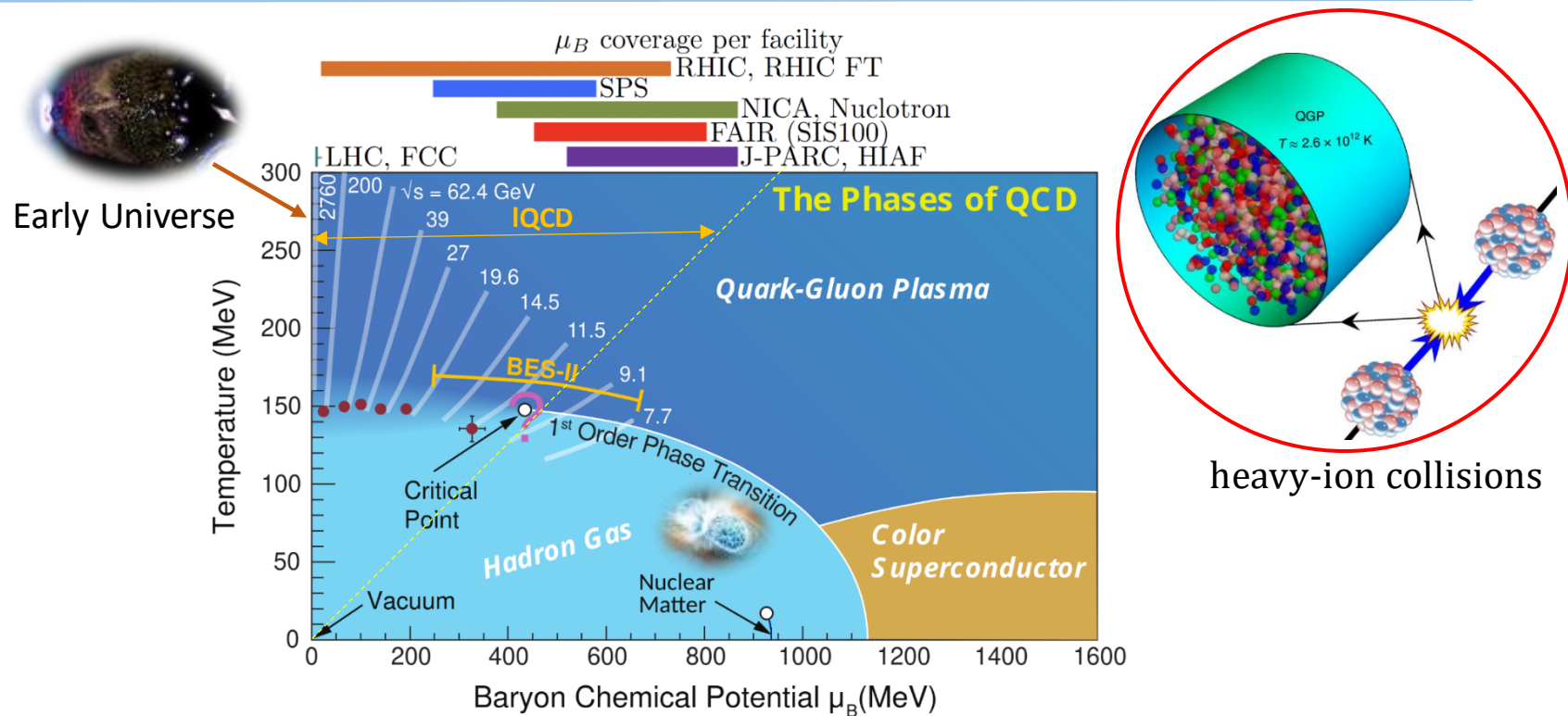


Motivation: the QCD phase diagram



- Explore the QCD phase diagram at finite T and μ_B through heavy-ion collisions
- Search for a possible Critical End Point (CEP) and 1st order **phase transition**
- Quantify macroscopic properties of the QCD matter at finite T and μ_B and relate them to its microscopic structures

Motivation: the QCD phase diagram



- Explore the QCD phase diagram at finite T and μ_B through heavy-ion collisions
- Search for a possible Critical End Point (CEP) and 1st order **phase transition**
- Quantify macroscopic properties of the QCD matter at finite T and μ_B and relate them to its microscopic structures

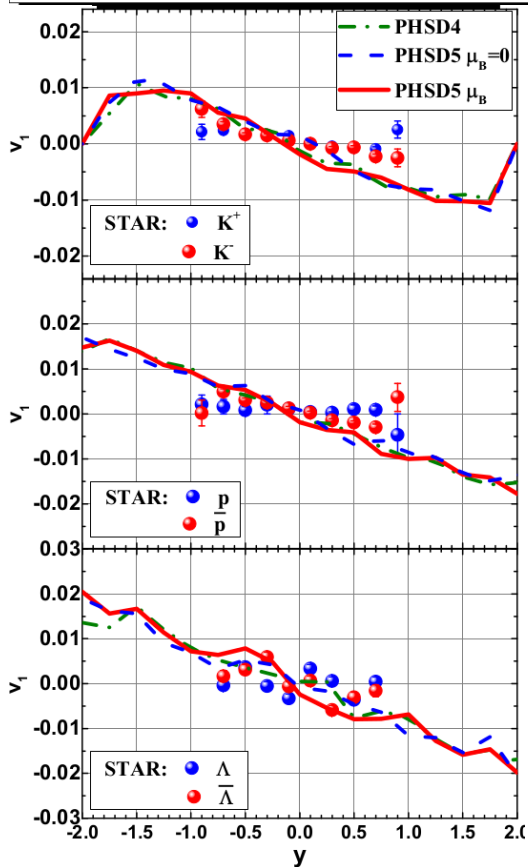
Directed flow ($\sqrt{s_{NN}} = 200 \text{ GeV vs } 27 \text{ GeV}$)

$$v_1 = \left\langle \frac{p_x}{p_T} \right\rangle$$

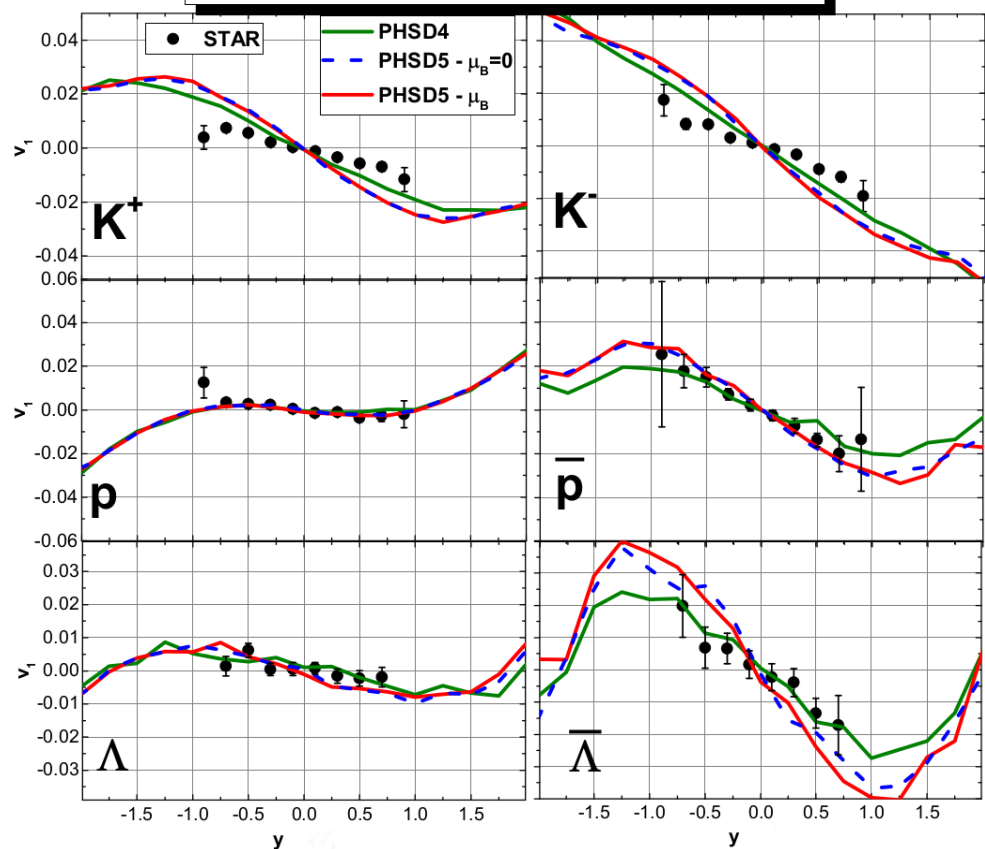
- Influence of the QGP dynamics on final particles observables
- Weak μ_B -dependence – **small** fraction of QGP or **low** μ_B

Particles 3 (2020)
no.1, 178-192

Au+Au $\sqrt{s_{NN}} = 200 \text{ GeV}$ 10-40% centrality



Au+Au $\sqrt{s_{NN}} = 27 \text{ GeV}$ 10-40% centrality

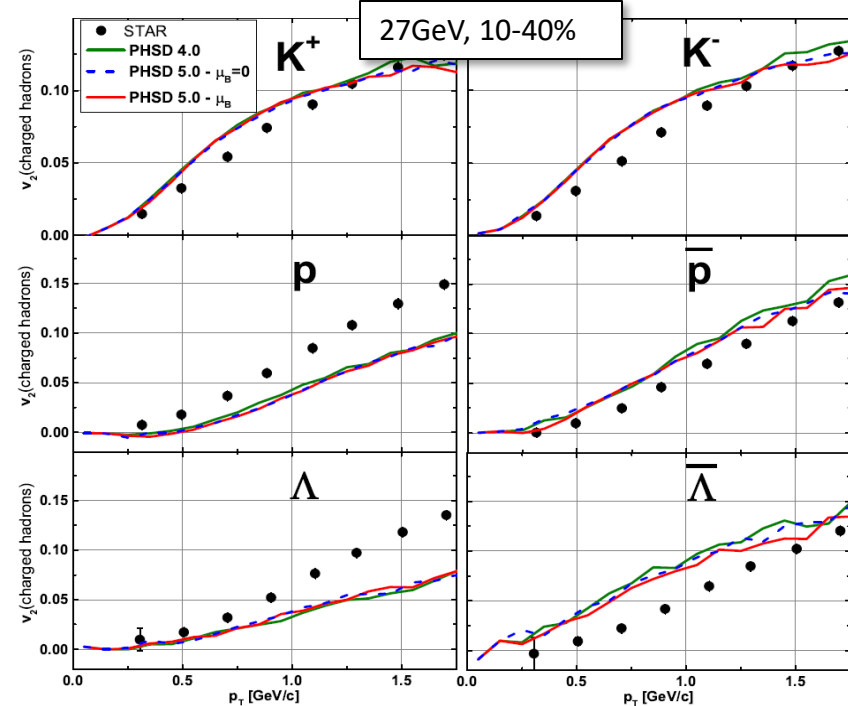
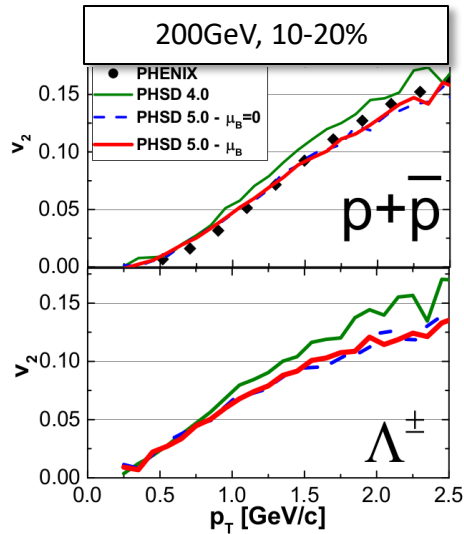


Elliptic flow ($\sqrt{s_{NN}} = 200 \text{ GeV vs } 27 \text{ GeV}$)

$$v_2 = \left\langle \frac{p_x^2 - p_y^2}{p_T^2} \right\rangle$$

- Weak μ_B -dependence
- Small effect of the angular dependence of $d\sigma/d\cos\theta$
- Strong flavor dependence

Particles 3 (2020)
no.1, 178-192



Channel decomposition :

